Characterizing magma fragmentation and its relationship with eruptive styles of Somma-Vesuvius volcano (Naples, Italy)

Manuscript Details

Manuscript number	VOLGEO_2019_161
Title	Characterizing magma fragmentation and its relationship with eruptive styles of Somma-Vesuvius volcano (Naples, Italy)
Article type	Research Paper

Abstract

Among the active volcanoes worldwide, Somma-Vesuvius, in Italy, is one with the highest volcanic risk as the surrounding areas are highly populated. Somma-Vesuvius is quiescent since 1944, but geological and historical records revealed a frequent violent explosive activity in the last 4000 years, representing a severe risk for the actual 700000 inhabitants living in the red zone (the area having a high probability for being impacted by pyroclastic density currents) and more than one million people who can be potentially affected by tephra fallout. This study aims at analysing the distribution of tephra fallout deposits and grain-size data from several Somma-Vesuvius eruptions of different styles, ranging from Violent Strombolian to sub-Plinian and Plinian, for characterizing the associated magmatic fragmentation through the assessment of the total grain-size distribution (TGSD). Chronologically, we focus on the Avellino (4365 BP) and Pompeii (A.D. 79) Plinian eruptions, Pollena (A.D. 472) sub-Plinian eruption, and the 1906 and 1944 Violent Strombolian eruptions. The related TGSDs were estimated by means of the Voronoi tessellation method, which, beside a suitable number of local grain-size distributions, requires the delimitation of the minimum tephra loading (zero-line contour). TGSDs for the different eruptive styles are needed by tephra dispersal models for reconstructing or predicting both tephra loading and airborne ash dispersal. However, due to the typical paucity of available field outcrops, field-derived TGSDs can be biased towards the coarse and fine populations. To encompass this issue, we performed a sensitivity study on the assumption behind TGSD reconstruction and described TGSD through analytical distributions, which best fit the field TGSDs. Our main objective is a more robust estimation of the TGSDs associated with the different eruptive styles. Characterizing such TGSDs, and the other eruption source parameters, is crucial for robustly predicting tephra loading and airborne ash dispersal of future eruptions at Somma-Vesuvius.

Keywords	Total grain-size distribution; Bulk granulometry; Eruption source parameters; Tephra fallout; Volcanic hazards assessment

Corresponding Author	Matthieu Poret
Corresponding Author's Institution	Istituto Nazionale di Geofisica e Vulcanologia
Order of Authors	Matthieu Poret, Miriana Di Donato, Antonio Costa, Roberto Sulpizio, Daniela Mele, Federico Lucchi
Suggested reviewers	Daniele Andronico, mauro antonio di vito, Guido Giordano, Bruce Houghton

Submission Files Included in this PDF

File Name [File Type]

Cover Letter.pdf [Cover Letter]

Highlights.docx [Highlights]

Poret_et_al_v3.2.docx [Manuscript File]

Submission Files Not Included in this PDF

File Name [File Type]

Fig. 1 - Context.png [Figure]

Fig. 2 - GSD - Avellino.png [Figure]

Fig. 3 - GSD - Pollena.png [Figure]

Fig. 4 - GSD - 1906.png [Figure]

Fig. 5 - GSD - 1944.png [Figure]

Fig. 6 - TGSD.png [Figure]

Table S1.xlsx [Table]

Table S2.xlsx [Table]

Table S3.xlsx [Table]

Table S4.xlsx [Table]

To view all the submission files, including those not included in the PDF, click on the manuscript title on your EVISE Homepage, then click 'Download zip file'.

Dr. Matthieu Poret
Laboratoire Magmas et Volcans
63000 Clermont-Ferrand
France
matthieu.poret@gmail.com

Dear Executive Editor,

Please find enclosed the manuscript entitled “Characterizing magma fragmentation and its relationship with eruptive styles of Somma-Vesuvius volcano (Naples, Italy)” by Matthieu Poret, Miriana Di Donato, Antonio Costa, Roberto Sulpizio, Daniela Mele, and Federico Lucchi to be considered for publication in Journal of Volcanology and Geothermal Research. Our work provides an assessment of the total grain size distributions (TGSD) on the basis of field data analysis for different eruptions of Somma-Vesuvius, helping to characterize magma fragmentation for the different eruptive styles analysed (i.e. from Violent Strombolian to Plinian). We focused on the Avellino and Pompeii Plinian eruptions, the Pollena sub-Plinian eruption, and the 1906 and 1944 Violent Strombolian eruptions.

For achieving this aim, we analysed field-data from the literature together with new data for assessing georeferenced grain size distributions at sites representative of the proximal, medial, and distal areas. By means of this dataset, we estimated the TGSDs for the Avellino, Pollena, 1906, and 1944 eruptions. We also studied the sensitivity of the Voronoi tessellation method used for such reconstructions. Although the number of tephra samples is limited, it covers proximal, medial, and distal areas, providing the current best approximations of the TGSDs relative to each eruption. TGSDs obtained through the Voronoi tessellation method were also estimated by means of analytical distributions (i.e. as sum of i) two lognormal and ii) two Weibull distributions), which allow for extrapolating field TGSDs. By comparing the TGSDs associated with the different eruptive styles, our results indicate that increasing the eruption intensity, i.e. going from Violent Strombolian to Plinian eruptive style, and the efficiency of magma fragmentation also increases. Moreover, they also show the significance of magma-water interaction on the amount of fines of the reconstructed TGSDs.

We hope you will find this study interesting and we believe that our results stimulate further works focussing on better characterizing TGSDs of other volcanic eruptions worldwide. In particular, the estimates of the TGSD for each eruption, representative of Violent Strombolian, sub-Plinian and Plinian styles, can be used as input for numerical models aimed at reconstructing past eruptions or tephra hazard assessment for similar scenarios.

On behalf of all co-authors, we declare no competing financial interests.

We hope that the content of this article will be of a broad interest to the Journal of Volcanology and Geothermal Research.

We are looking forward to your editorial decision.

Yours sincerely,

Matthieu Poret

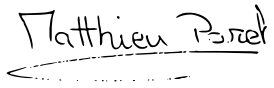

Highlights

1 Tephra deposits of 4 different eruptions of Vesuvius were analyzed

2 Deposit volumes and bulk granulometries were reconstructed from field data analysis

3 Performed comparative study for different eruption and magma fragmentation styles

4 Results are important for tephra dispersal modelling and hazard assessment purposes

Characterizing magma fragmentation and its relationship with eruptive styles of Somma-Vesuvius volcano (Naples, Italy)

Matthieu Poret [1*], Miriana Di Donato [2], Antonio Costa [1], Roberto Sulpizio [3], Daniela Mele [3], and Federico Lucchi [2]

[1] Université Clermont Auvergne, CNRS, IRD, OPGC, Laboratoire Magmas et Volcans, Clermont-Ferrand, France
[2] Università di Bologna, Dipartimento di Scienze Biologiche, Geologiche e Ambientali, Bologna, Italy
[3] Università di Bari, Dipartimento di Scienze della Terra e Geoambientali, Bari, Italy
* Corresponding author e-mail: matthieu.poret@gmail.com

Abstract

Among the active volcanoes worldwide, Somma-Vesuvius, in Italy, is one with the highest volcanic risk as the surrounding areas are highly populated. Somma-Vesuvius is quiescent since 1944, but geological and historical records revealed a frequent violent explosive activity in the last 4000 years, representing a severe risk for the actual 700000 inhabitants living in the red zone (the area having a high probability for being impacted by pyroclastic density currents) and more than one million people who can be potentially affected by tephra fallout. This study aims at analysing the distribution of tephra fallout deposits and grain-size data from several Somma-Vesuvius eruptions of different styles, ranging from Violent Strombolian to sub-Plinian and Plinian, for characterizing the associated magmatic fragmentation through the assessment of the total grain-size distribution (TGSD). Chronologically, we focus on the Avellino (4365 BP) and Pompeii (A.D. 79) Plinian eruptions, Pollena (A.D. 472) sub-Plinian eruption, and the 1906 and 1944 Violent Strombolian eruptions. The related TGSDs were estimated by means of the Voronoi tessellation method, which, beside a suitable number of local grain-size distributions, requires the delimitation of the minimum tephra loading (zero-line contour). TGSDs for the different eruptive styles are needed by tephra dispersal models for reconstructing or predicting both tephra loading and airborne ash dispersal. However, due to the typical paucity of available field outcrops, field-derived TGSDs can be biased towards the coarse and fine populations. To encompass this issue, we performed a sensitivity study on the assumption behind TGSD reconstruction and described TGSD through analytical distributions, which best fit the field TGSDs. Our main objective is a more robust estimation of the TGSDs associated with the different eruptive styles. Characterizing such TGSDs, and the other eruption source parameters, is crucial for robustly predicting tephra loading and airborne ash dispersal of future eruptions at Somma-Vesuvius.

Keywords: Total grain-size distribution; Bulk granulometry; Eruption source parameters; Tephra fallout; Volcanic hazards assessment

1 Introduction

The Somma-Vesuvius volcanic complex is one of the most studied volcanoes in the world, and is included among the highest volcanic risks in the world (e.g. Macedonio et al., 2008). One of the main goals of modern volcanology is a quantitative assessment of volcanic hazards (e.g. tephra loading, airborne ash dispersal) in sensitive areas like those surrounding Somma-Vesuvius, where they can heavily impact the metropolitan city of Naples (Italy) with potential severe consequences for the central Mediterranean zone (Folch and Sulpizio, 2010; Sulpizio et al., 2014). For a robust volcanic hazard assessment, we must know the eruptive history of the volcano and its past behaviour (e.g. Cioni et al., 2008; Santacroce et al., 2008). Such information derives typically from the analysis of geological records (e.g. Cioni et al., 1999; 2008; Santacroce and Sbrana, 2003; Santacroce et al., 2008; Gurioli et al., 2010; Sulpizio et al., 2010a; 2010b; 2010c; 2010d; 2014). In fact, analysis of geological data allows assessing the key eruption source parameters (ESP) associated with an eruption, such as the total erupted mass (TEM; i.e. eruption magnitude), mass eruption rate (MER; i.e. eruption intensity), eruptive column height, and total grain-size distribution (TGSD), which depends on the intensity and behaviour of the initial magma fragmentation (Bonadonna and Houghton, 2005; Bonadonna et al., 2015; Costa et al., 2016). To investigate the effect of different magma compositions and eruption intensity on ESPs, we selected four eruptions from the eruptive record of Somma-Vesuvius, representative of its most frequent eruptive styles. In particular, we considered the Avellino Plinian eruption (c.a. 3900 years BP; Sevink et al., 2011), the Pollena sub-Plinian eruption (A.D. 472; Sulpizio et al., 2005; Santacroce et al., 2008; Foch and Sulpizio, 2010), and the Violent Strombolian eruptions of 1906 (Mercalli, 1906; Arrighi et al., 2001) and 1944 (Imbò, 1949; Cubellis et al., 2013). Moreover, for comparison purposes, we also considered the TGSD of the Pompeii Plinian eruption (A.D. 79) derived from Macedonio et al. (1988; 2008). The literature reports petrochemical and lithological features of the tephra deposits for these four eruptions (e.g. Imbò, 1949; Macedonio et al., 1988; Arrighi et al., 2001; Cioni et al., 1999; 2003a; 2003b; 2004; 2008; Sulpizio et al., 2005; 2007; 2008; 2010a; 2010b; 2010c; 2010d; 2012; 2014; Cole and Scarpati, 2010; Cubellis et al., 2013; Barsotti et al., 2015).

This study aims at bringing together geological data from different eruptions of different styles at Somma-Vesuvius to assess and compare the relative magma fragmentation processes, and characterize their ESPs, which is pivotal for robustly predicting tephra loading and airborne ash dispersal of future eruptions. Moreover, the quantification of TGSD, including ash, for each eruption can be used as an indicator for comparing the magma fragmentation efficiency during the different eruptions, and its effect on the eruptive style at Somma-Vesuvius.

Assessing TGSD is also very important for characterizing the eruptive style by associating particle size distribution to the initial gas content and magma-water interaction processes (e.g. Kaminski and Jaupart, 1998, Rust and Cashman, 2011, Costa et al., 2016). Commonly, TGSD is required as key input parameter within tephra dispersal models for reconstructing or predicting the tephra loading and airborne ash dispersal (e.g. Folch, 2012), and to produce risk mitigation strategies (Folch et al., 2008; Scollo et al., 2008) for future eruptions (e.g. at Somma-Vesuvius). In this study, the TGSDs of the Avellino, Pollena, 1906, and 1944 eruptions, from Plinian to sub-Plinian and Violent Strombolian, are assessed by means of the Voronoi tessellation method (Bonadonna and

Houghton, 2005), which integrates individual georeferenced grain-size distributions (GSD) for each eruption. We also focussed on estimating the fraction of particle matter finer than 10 μm (hereinafter PM_{10}) numerically needed for assessing the content of airborne ash (Poret et al., 2018b), which can potentially affect aviation (e.g., Folch and Sulpizio, 2010; Folch et al., 2012; Sulpizio et al., 2012).

However, determining TGSD from field samples analysis only can have strong limitations due to the sampling distance from the vent (Costa et al., 2016; Poret et al., 2018b) and the spatial and density distribution of samples along the main axis of the tephra plume (Bonadonna and Houghton, 2005; Bonadonna et al., 2015; Spanu et al., 2016). In fact, field-derived TGSD typically tends to underestimate the fraction of either or both the coarse and fine populations (Bonadonna and Houghton, 2005; Rose and Durant, 2009; Scollo et al., 2014; Costa et al., 2016). For encompassing these issues and assessing the related uncertainties we carried out a sensitivity analysis and also described the TGSD as the sum of two lognormal (Gaussian in Φ) and then two Weibull distributions by best fitting the field-based TGSDs (Costa et al., 2016, 2017; Poret et al., 2017; 2018b; Mueller et al., 2019; Pedrazzi et al., 2019).

This paper presents first a brief description of the eruptive history of the Somma-Vesuvius volcano, summarizing the main features of each of the considered eruptions. Then, we report the data and methodology used to estimate the relative TGSDs. Finally, we show the TGSD obtained for each eruption together with the discussion of the main findings.

2 Eruptive history summaries of Somma-Vesuvius and selected eruptions

The Somma-Vesuvius eruptive history showed alternating effusive and explosive eruptions, sometimes associated with destructive phases (caldera) of the volcanic edifice. In particular, four Plinian eruptions with caldera collapses truncated the Mt. Somma volcano, forming the present-day summit caldera (Cioni et al., 1999; 2008; Rolandi et al., 2004; Santacroce et al., 2008). Chronologically, these are the Pomici di Base (22.03 ± 0.18 cal ky BP; Bertagnini et al., 1998; Santacroce et al., 2008), Mercato (8.89 ± 0.09 cal ky BP; Santacroce et al., 2008; Mele et al., 2011), Avellino (3.90 ± 0.04 cal ky BP; Sevink et al., 2011; Sulpizio et al., 2010), and Pompeii (A.D. 79; Sigurdsson et al., 1985) eruptions. After the Pompeii eruption, the Vesuvius cone started to grow within the Mt. Somma caldera reaching its present shape (Cioni et al., 2008). Nonetheless, among the recorded post-Pompeii activities, several high-intensity explosive eruptions occurred at Somma-Vesuvius partly modifying the structure of the cone. These are the sub-Plinian Pollena (A.D. 472; Sulpizio et al., 2005) and A.D. 1631 (Poret et al., 2019) eruptions. The most recent period of activity (between A.D. 1631–1944) was characterised by recurrent summit and lateral lava effusions associated with semi-persistent and mild explosive activity, interrupted by pauses lasting from months to a maximum of seven years (Santacroce, 1987; Cioni et al., 2008). During this period, Vesuvius produced a few Violent Strombolian eruptions, such as in 1906 and 1944. In terms of eruption magnitudes (i.e. erupted volume), the literature for the Somma-Vesuvius eruptions reports volumes ranging from 1 to 10 km^3 for Plinian, 0.01 to 1 km^3 for sub-Plinian, and 0.001 to 0.01 km^3 for Violent Strombolian eruptions (Cioni et al., 2008).

Hereinafter, we report a synthetic description of the main features of the eruptions considered in the present study.

2.1 Avellino and Pompeii Plinian eruptions

The Avellino eruption (3.90 ± 0.04 cal ky BP; Sevink et al., 2011), was subdivided in three eruptive phases: opening, magmatic Plinian, and phreatomagmatic (Sulpizio et al., 2010b; 2010c; Massaro et al., 2018). During the opening phase, a transient short-lived eruptive column reached 12-20 km, followed by the formation of pyroclastic density currents (PDC) from partial or total collapse of the eruptive column (Sulpizio et al., 2010c). The magmatic Plinian phase produced a sustained eruptive column growing with time from 22 to 30 km. This phase ejected the main volume of tephra estimated at 1.4 km^3, which was dispersed mostly north-eastwards (Cioni et al., 2003a; Sulpizio et al., 2008; 2010c). Finally, the phreatomagmatic phase was dominated by PDC deposits, which significantly contributed to the total erupted volume with ~1 km^3 (Sulpizio et al., 2008; 2010a; 2014; Gurioli et al., 2010). It is worth noting that tephra from the Plinian phase was recovered as far as in Albania (Fig. 1), where they occur within the sedimentary succession of Shkodra lake (~430 km from the source; Sulpizio et al., 2010a).

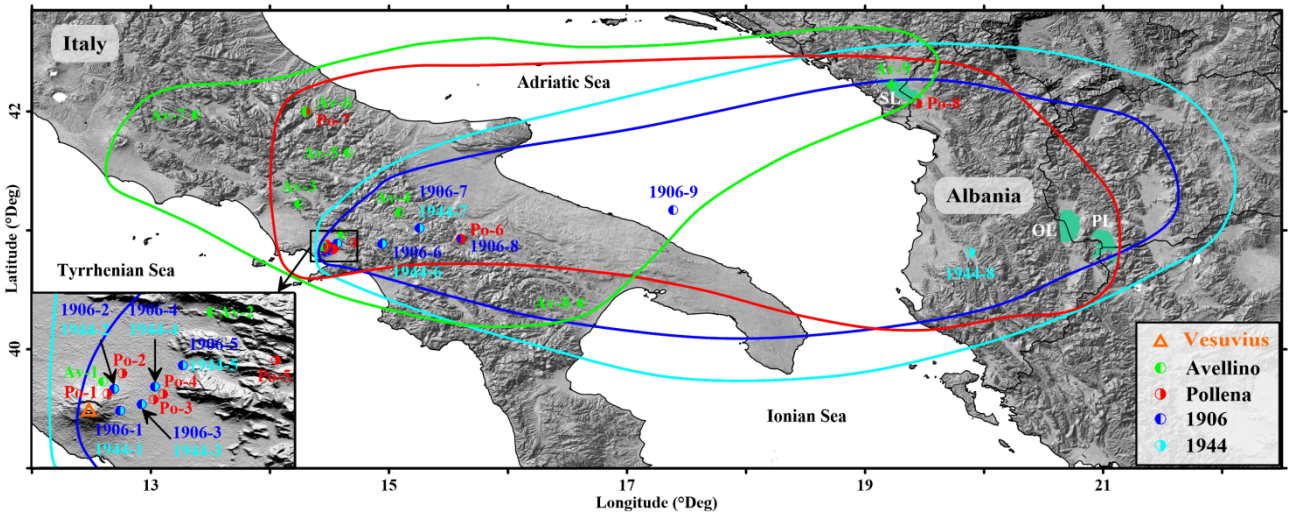

Fig. 1: Map of the main outcrops of the Avellino, Pollena, 1906, and 1944 Somma-Vesuvius eruptions. The left-bottom inset zooms onto the proximal area. Coloured lines refer to the dispersal area for each eruption, modified after Sulpizio et al., 2010a, 2010b; 2010c; 2014 for Avellino; Sulpizio et al., 2005; 2010a; 2014 for Pollena; Arrighi et al., 2001; Barsotti et al., 2015 for 1906; and Imbò, 1949; Cole and Scarpati, 2010; Cubellis et al., 2013 for 1944. SL, OL, and PL refer respectively to the Shkodra, Ohrid, and Prespa lakes (Albania and FYROM). For the interpretation of the references to colour in this figure legend, the reader is referred to the web version of this article.

Concerning the Pompeii (A.D. 79) Plinian eruption of Somma-Vesuvius, very famous for the destruction of the Roman towns of Pompeii and Herculaneum, the volcanological aspects have been described by numerous authors (e.g. Sigurdsson et al., 1985, Carey and Sigurdsson, 1987, Macedonio et al., 1988; Pfeiffer et al., 2005). After a short initial phreatomagmatic vent-opening phase, the eruption was characterized by a purely magmatic phase with a high sustained eruption column, which was subdivided into a lower layer of white phonolitic pumice (White Pumice) and an upper tephritic–phonolitic pumice fall (Gray Pumice) deposit. This phase ended column collapse and the emplacement of pyroclastic flows, which was followed by phreatomagmatic activity and the emplacement of lithic-rich breccia and pyroclastic surges, interpreted as the consequence of decreasing pressure in the vent and magma–water interaction. For the White and the Gray units,

Sigurdsson et al. (1985) estimated, respectively, 2.5×10^{12} and 6.5×10^{12} kg of tephra, or 1 and 2.6 km^3 DRE. Concerning the column height, they estimated that during the White Pumice phase it increased from about 15 to 26 km, while during the Gray phase, it reached to a maximum of 32 km and then decreased to about 27 km.

2.2 Pollena sub-Plinian eruption

The Pollena eruption (A.D. 472) is the major sub-Plinian event of Somma-Vesuvius, and is considered by Italian Civil Protection as one of the reference scenarios in case of renewal of explosive activity. Sulpizio et al. (2005) described the eruption through three phases (i.e. opening, magmatic and phreatomagmatic), with a similar eruptive evolution to that described for the Plinian events. In particular, the Pollena eruption was characterized by a highly unstable MER during the opening phase, resulting in eruptive column pulses with general dispersal of the tephra fallout deposit towards north-east. Then, during the magmatic phase, at least two dominant pulses of high eruptive intensity are recorded by the deposition of pyroclastic fall beds and by the signature of dilute and dense PDCs (Sulpizio et al., 2005). The MER reached a peak intensity of ~3.4×10^7 kg/s during this phase, in particular during the emplacement of the L_8 fallout bed, which is the most dispersed (Sulpizio et al., 2005). The final phreatomagmatic phase was characterized by a pulsating column and emplacement of diluted to concentrated PDCs.

The tephra fallout deposits dispersed north-eastwards (Fig. 1; see also Sulpizio et al., 2005), while the PDCs deposited mainly on the northern slopes of the volcano. It is worth noting that fine ash reached the Balkans, being identified in the sedimentary succession of the Shkodra lake (~440 km from the source; Sulpizio et al., 2010a), and as crypto-tephra in Ohrid lake (Sulpizio et al., 2010c). Sulpizio et al. (2005) estimated the volume of the pyroclastic fall deposits around 0.44 km^3 using the proximal isopachs. Such a volume increases up to ~1.38 km^3 and the maximum column height around 28 km by adding data from distal sites (Sulpizio et al., 2005).

2.3 The 1906 and 1944 Violent Strombolian eruptions

The 1906 and 1944 eruptions are examples of Violent Strombolian eruptions at Somma-Vesuvius, which are typically characterized by emplacement of lava flows in the early phases followed by explosive activities (Imbò, 1949; Cioni et al., 2008). The latter phases of the eruptions typically consist of intense lava fountaining episodes associated with eruptive columns rising up to several kilometre heights. Sometimes, a phreatomagmatic phase closed the activity, accompanied by ash emissions. The Violent Strombolian eruptive style is considered the most likely scenario in the case of a possible future reactivation of Somma-Vesuvius (Marzocchi et al., 2004; Neri et al., 2008). In particular, the eruptions of 1906 and 1944 produced tephra deposits of metric thickness in proximal areas, with distal ash deposits recognized as far as in Albania (Cubellis et al., 2013).

Several overviews and details of the 18-day long 1906 eruption are available in the literature (e.g. De Lorenzo, 1906; Mercalli, 1906; Sabatini, 1906; Perret, 1924; Bertagnini et al., 1991; Scandone et al., 1993; Barsotti et al., 2015). The eruption started with a 4-day effusive-explosive phase; then an intense lava fountaining episode occurred and the Violent Strombolian phase started, lasting 2 days (Mercalli, 1906; Barsotti et al., 2015 – Phase I) and producing a column that reached ~13 km

above the vent (Perret, 1924; Scandone et al., 1993). Ash emissions dispersed towards the Adriatic Sea (Arrighi et al., 2001) and Montenegro (~400 km from the vent; De Lorenzo, 1906; Barsotti et al., 2015), as shown by the tephra fallout extent displayed in Fig. 1. Finally, a 12-day long phases of ash emission (Barsotti et al., 2015 – Phase II) occurred releasing abundant reddish-grey fine ash together with millimetre-sized accretionary lapilli (De Lorenzo, 1906; Mercalli, 1906). Wind conditions alternatively dispersed ash over the city of Naples and surroundings (Hobbs 1906). Sabatini (1906) estimated a minimum tephra fallout volume of ~0.21 km^3 and Barsotti et al. (2015) reported a TEM of 1.34×10^{11} kg. Furthermore, they mention a MER of 10^6 and 10^5 kg/s for Phase I and II respectively, i.e. a bulk MER of 10^6 kg/s. Sulpizio et al. (2012) estimated a TEM at 9.3×10^{10} kg and a fallout mass of 3.7×10^{10} kg. For a duration of 18 days, the average MER is estimated at 6×10^4 kg/s. In contrast, Cioni et al. (2008; references therein) report a peak MER of 3.4×10^5 kg/s for the basal lapilli bed and 5.4×10^6 kg/s for the paroxysmal phase.

The 17-day long 1944 eruption started with the emplacement of lava flows mainly towards the north slopes of the actual Vesuvius cone. The subsequent explosive phase comprises a series of 8 lava fountains over a time interval of ~8 h (Arrighi et al., 2001). Scandone et al. (1993) report for this phase a steady eruptive column that reached ~5 km above the vent and ejected ash into the atmosphere (Macedonio et al., 2008). In particular, Imbò (1949) provided information relative to the meteorological conditions. The tephra was transported towards south-east (Fig. 1), reaching Albania where ash fallout has been observed in Devoli (Cubellis et al., 2013). Cioni et al. (2008) estimated the erupted volume at ~0.066 km^3 from the isopachs map produced by Pesce and Rolandi (2000). Based on the TEM estimated at 2.2×10^{12} kg and the eruption duration (17 days), the average MER is estimated at 1.5×10^6 kg/s (Cioni et al., 2008). Differently, Scandone et al. (1986) report a MER of 4×10^5 kg/s, whereas Macedonio et al. (2008) estimated the MER at 5×10^5 kg/s for modelling tephra fallout.

3 Data and Methodology

3.1 Field data

To reconstruct the dispersal of tephra deposits of the studied eruptions (Fig. 1), we used geological data from literature (e.g. Imbò, 1949; Arrighi et al., 2001; Cioni et al., 2003a; Sulpizio et al., 2005; 2007; 2010a; 2010b; 2010c; 2010d; 2012; 2014; Cole and Scarpati, 2010; Cubellis et al., 2013; Barsotti et al., 2015). Throughout the manuscript, we will use the terms proximal, medial, and distal for indicating the areas affected by tephra at different distances. Nonetheless, these zones reflect the distance from the vent and strongly depend on the eruption intensity (i.e. the column height) together with the atmospheric conditions (e.g. wind fields). Costa et al. (2016) proposed to consider distances from 1/10 to 10 times the eruptive column height to define the proximal, medial, and distal deposits, for adequately sampling the whole tephra fallout up to 125 μm (although such distances depend on wind conditions as discussed in their work). In this study, for the sake of simplicity, we use the term proximal to indicate distances from the source up to 30 km, medial for distances of 30-200 km, and distal for distances > 200 km.

Field data comprise tephra samples collected for the Avellino, Pollena, 1906, and 1944 eruptions (Fig. 1; Table 1). All the details are available as Supplementary Material (Tables S1, S2, S3, and S4

respectively for the Avellino, Pollena, 1906, and 1944 eruptions). Regarding the Avellino eruption, we used 9 samples distributed from proximal (samples 1-2), to medial areas (samples 3-8) derived from Sulpizio et al. (2010b), and a distal one in the Shkodra lake (sample 9; Sulpizio et al., 2010a). The Pollena fallout deposits were characterized using 8 samples distributed in proximal (samples 1-5), medial (samples 6-7), and distal areas (sample 8 in the Shkodra lake, Albania; Sulpizio et al., 2010a). Recently, ash related to the Pollena eruption was also reported as crypto-tephra in the Ohrid lake (Albania and FYROM border; Vogel et al., 2009; Sulpizio et al., 2010d), expanding significantly the tephra deposit eastwards (Fig. 1). However, the lack of grain-size analysis prevents from integrating data for this outcrop.

Table 1: Field measurements (i.e. location, distance from the vent, main mode, and loading) used for the grain-size analysis and TGSD estimations of the Avellino, Pollena, 1906, and 1944 eruptions at Somma-Vesuvius. Sample locations are shown in Fig. 1. Details of the field data are available as Supplementary Material (Tables S1, S2, S3, and S4).

Samples	**Field observations**				
Avellino	**Longitude**	**Latitude**	**Distance (km from source)**	**Mode (Φ)**	**Loading (kg/m^2)**
Av-1	**14.447**	**40.867**	**5**	**-3**	**1.80×10^{2}**
Av-2	**14.611**	**40.971**	**23**	**-2**	**1.40×10^{2}**
Av-3	**14.245**	**41.223**	**47**	**3**	**3.00×10^{1}**
Av-4	**15.091**	**41.151**	**67**	**1**	**1.20×10^{2}**
Av-5	**14.661**	**41.654**	**94**	**2**	**4.00×10^{1}**
Av-6	**14.305**	**42.001**	**131**	**5**	**3.00×10^{1}**
Av-7	**13.385**	**41.974**	**155**	**4**	**3.00×10^{1}**
Av-8	**16.619**	**40.388**	**191**	**5**	**3.00×10^{1}**
Av-9	**19.232**	**42.228**	**430**	**5**	**1.00×10^{1}**
Pollena					
Po-1	**14.454**	**40.849**	**4**	**-3**	**3.84×10^{2}**
Po-2	**14.477**	**40.879**	**8**	**-2**	**1.30×10^{2}**
Po-3	**14.524**	**40.839**	**9**	**-3**	**1.40×10^{2}**
Po-4	**40.848**	**14.538**	**10**	**-3**	**1.30×10^{2}**
Po-5	**14.708**	**40.899**	**25**	**-1**	**1.68×10^{2}**
Po-6	**15.605**	**40.930**	**100**	**2**	**3.50×10^{1}**
Po-7	**14.305**	**42.001**	**130**	**3**	**1.00×10^{1}**
Po-8	**19.440**	**42.070**	**440**	**6**	**5.00×10^{1}**
1906					
1906-1	**14.473**	**40.823**	**4**	**-2**	**5.50×10^{2}**
1906-2	**14.464**	**40.856**	**5**	**-2**	**5.50×10^{2}**
1906-3	**14.506**	**40.833**	**7**	**0**	**2.75×10^{2}**
1906-4	**14.526**	**40.859**	**10**	**-2**	**1.10×10^{2}**
1906-5	**14.567**	**40.891**	**14**	**-3**	**1.10×10^{2}**
1906-6	**14.946**	**40.887**	**44**	**1**	**1.10×10^{1}**
1906-7	**15.258**	**41.019**	**72**	**2**	**5.50×10^{0}**
1906-8	**15.605**	**40.931**	**100**	**3**	**2.20×10^{0}**
1906-9	**17.388**	**41.173**	**252**	**3**	**4.40×10^{0}**
1944					
1944-1	**14.473**	**40.823**	**4**	**-2**	**6.00×10^{2}**
1944-2	**14.464**	**40.856**	**5**	**-2**	**6.00×10^{2}**
1944-3	**14.506**	**40.833**	**7**	**-1**	**3.00×10^{2}**
1944-4	**14.526**	**40.859**	**10**	**-1**	**1.20×10^{2}**
1944-5	**14.567**	**40.891**	**14**	**-3**	**1.00×10^{1}**
1944-6	**14.946**	**40.887**	**44**	**1**	**1.20×10^{1}**
1944-7	**15.258**	**41.019**	**72**	**2**	**6.00×10^{0}**
1944-8	**19.883**	**40.814**	**460**	**5**	**1.20×10^{0}**

For the 1906 and 1944 Violent Strombolian eruptions, 7 samples were collected at the same locations (Table 1), representing the proximal (samples 1-5) and medial areas (samples 6-7). Then, the samples 8 and 9 of the 1906 eruption were collected in the Monticchio lake and in a marine core offshore the city of Bari (Fig. 1), located at ~100 and ~252 km from the source respectively. The data related to these samples are reported in Fig. 1 and Table 1. For the 1944 eruption, the farthest sample (sample 8) was collected in Devoli (Albania; Cubellis et al., 2013), which is ~460 km from the vent.

3.2 Estimating the TGSDs

Sampling data include measurements of the tephra loading at several sites (Fig. 1 and Table 1), which were sieved for assessing the GSDs relative to the affected areas. The sieving method gives GSD from -5 to 5 Φ (Poret et al., 2018a), where $\Phi = -\log_2 d$ with d is the particle diameter in millimetre (Krumbein, 1934). Meanwhile, fine ash was analysed through the Beckman Coulter Counter Multisizer™ 4 at the University of Bari, Italy. The latter method gives GSD from 3 to 7 Φ, extending the grain-size analysis towards the tail of the distribution relative to fine ash. The resulting normalized GSD is obtained by integrating the two partial GSDs taking the sieving method as reference. A similar procedure was successfully used in Poret et al. (2018b) for grain-size purposes integrating complementary methods. Each GSD includes tephra information relative to the bombs (or blocks; diameter $d \geq 64$ mm), lapilli (2 mm $\leq d <$ 64 mm), and ash ($d <$ 2 mm). We further distinguish coarse ash, 64 μm $\leq d <$ 2 mm, and fine ash, $d <$ 64 μm (e.g., Folch, 2012).

Among the several integration methods existing for estimating TGSD (e.g. weighted average, Walker et al., 1981; sectorization of the deposit, Carey and Sigurdsson, 1982; isomass maps, Murrow et al., 1980), in this study we use the Voronoi tessellation method (Bonadonna and Houghton, 2005), considering its advantages and limitations (Bonadonna and Houghton, 2005; Bonadonna et al., 2015; Costa et al., 2016; Spanu et al., 2016; Poret et al., 2018a; 2018b). The method consists in dividing the pyroclastic deposit into Voronoi polygons associated with each georeferenced GSD (i.e. each sample). Then, TGSD is obtained as the weighted average of the mass distribution over the Voronoi cells, which refer to the entire deposit. Prior to apply this method, it is fundamental to define the areal extent of the tephra deposit through assessment of the zero-line contour, which is the line at which the deposit thickness can be assumed negligible (literally equal to zero; Bonadonna and Houghton, 2005). In the studied cases, we used the data from the literature to assess the zero contours (see Fig. 1). Starting from the field-based TGSDs of the different eruptions, we also inferred the TGSDs by means of general analytical distributions (Costa et al., 2016; 2017). First, we considered the sum of two lognormal distributions (hereinafter bi-Gaussian in Φ-units):

$$f_{bi-Gaussian}(\Phi) = p\frac{1}{\sigma_1\sqrt{2\pi}}e^{-\frac{(\Phi-\mu_1)^2}{2\sigma_1^2}} + (1-p)\frac{1}{\sigma_2\sqrt{2\pi}}e^{-\frac{(\Phi-\mu_2)^2}{2\sigma_2^2}} \quad (271)$$

where Φ denotes particle diameter, p and (1-p) are, respectively, the coarse and fine sub-population weights, and μ_1, μ_2 and σ_1, σ_2 denote the mean and standard deviation of the two Gaussian distributions in Φ-units. Then, we used two Weibull distributions (Costa et al., 2016; 2017):

$$f_{bi-Weibull}(d) = q\frac{1}{n_1^{\frac{1}{n_1}}\Gamma\left(1+\frac{1}{n_1}\right)}\frac{1}{\lambda_1}\left[\frac{d}{\lambda_1}\right]^{n_1} e^{-\frac{1}{n_1}\left(\frac{d}{\lambda_1}\right)^{n_1}} + (1-q)\frac{1}{n_2^{\frac{1}{n_2}}\Gamma\left(1+\frac{1}{n_2}\right)}\frac{1}{\lambda_2}\left[\frac{d}{\lambda_2}\right]^{n_2} e^{-\frac{1}{n_2}\left(\frac{d}{\lambda_2}\right)^{n_2}} \quad (275)$$

where d denotes particles diameter, q and (1-q) are, respectively, the coarse and fine sub-population weights, and λ_1, λ_2 and n_1, n_2 are the scale and shape parameters of the two distributions.

4 Results and discussions

4.1 Individual grain-size distributions

The results for the individual GSDs are displayed in Figs. 2, 3, 4 and 5, respectively for the Avellino, Pollena, 1906, and 1944 eruptions. First of all, it is worth noting that all the TGSD reconstructions (Fig. 6) reflect the limitations associated with the available tephra samples in terms of number and spatial distribution. Moreover, such a reconstruction suffers from the fact that all kinds of tephra particles are considered together, without distinguishing for the different lithologies, which can have different settling behaviours. However, the reconstructed TGSDs represent the best approximations of the initial magma fragmentation for each of the studied eruptions.

Regardless of the eruption, the GSDs at each location show a unimodal distribution with a clear shift of the mode from proximal to distal areas. Such features have been typically observed for several tephra fallout deposits (e.g. Durant et al., 2009; 2010 for the 1980 Mt. St. Helens eruption; Watt et al., 2015 for the Chaiten eruption). Considering the proximal samples (Fig. 1; Table 1), regardless of the eruption, the modes range from -3 to 0 Φ (Table 1), with similar size and proportions, indicating a dominancy of lapilli and coarse ash up to 30 km from the source, typically having relatively high terminal velocities, and thus depositing near the volcano (Bonadonna and Costa, 2013). Regarding the medial areas, the modes range from 1 to 6 Φ (Table 1), covering a larger grain-size range than in the proximal area due to a larger sampling distance range (i.e. ~44-191 km from the source), different eruptive column heights (3-30 km), and wind intensities (Costa et al., 2016). In particular, for the Pollena, 1906, and 1944 eruptions, the modes vary from 1 to 3 Φ (see Figs. 3, 4, 5, and Table 1), whereas the Avellino eruption has medial modes up to 6 Φ (Fig. 2 and Table 1). Indeed, only the Avellino eruption deposits have medial samples up to ~191 km from the vent. Furthermore, samples at similar distances from the source tend to indicate the same modes, being consistent with the main findings of Spanu et al. (2016). Considering the distal samples, modes range between 5 to 6 Φ, except for the 1906 distal sample (i.e. 3 Φ; Fig. 4 and Table 1), which is closer to the vent than for the other eruptions (i.e. ~252 km from the source instead of ~430-460 km). It is worth noting that the relative GSDs indicate a good preservation of the tephra fallout for the studied eruptions, mostly made of fine ash (including PM_{10}) collected beyond the Apennines and Adriatic Sea up to Albania and Montenegro (Fig. 1; Sulpizio et al., 2010a; 2010d).

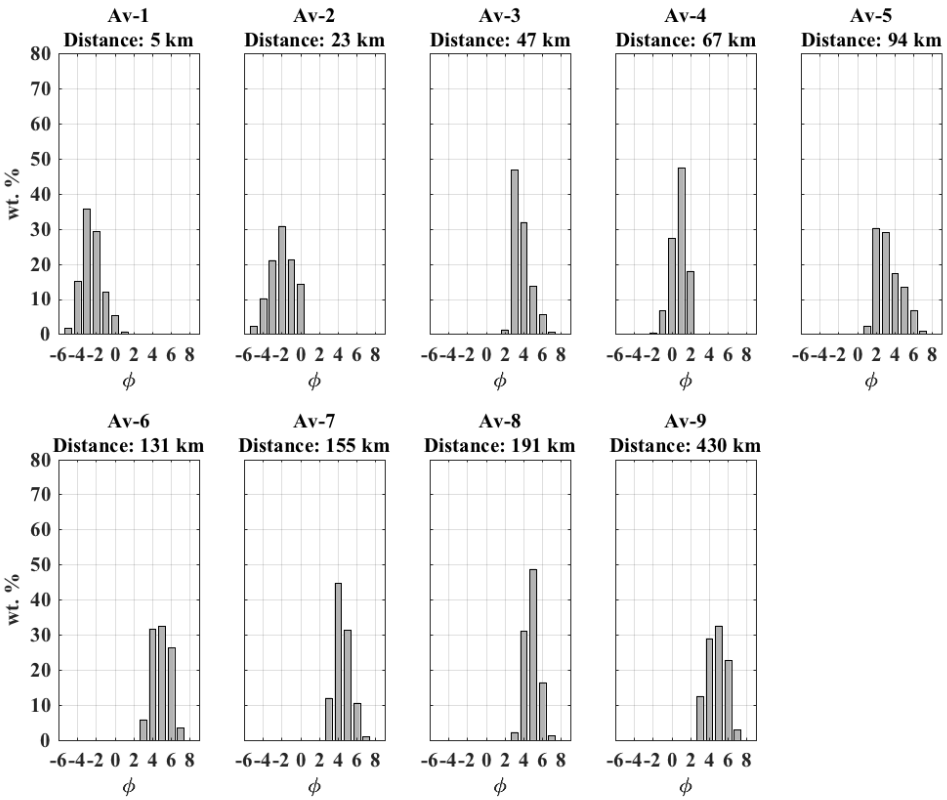

Fig. 2 Individual field-derived grain-size distributions (samples Av-x) for the Avellino Plinian eruption. Sample locations are shown in Fig. 1 and the relative details reported in Table 1. Details of the GSDs are available as Supplementary Material (Table S1).

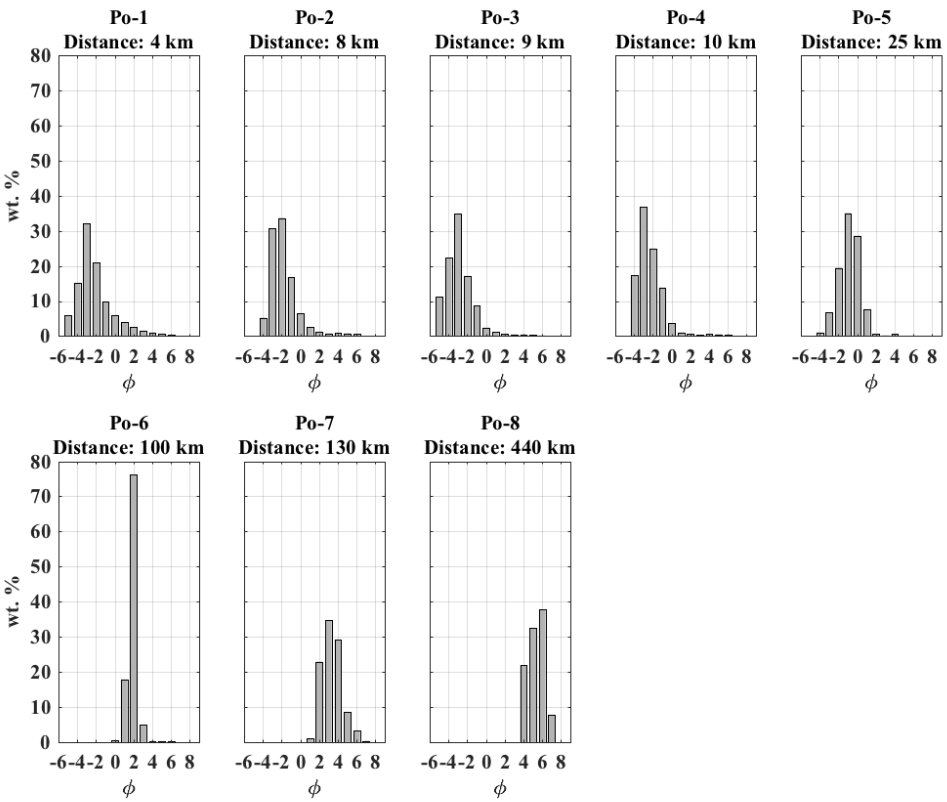

Fig. 3: Individual field-derived grain-size distributions (samples Po-x) for the Pollena sub-Plinian eruption. Sample locations are shown in Fig. 1 and the relative details reported in Table 1. Details of the GSDs are available as Supplementary Material (Table S2).

Considering the similarities observed in the evolution of the Plinian and sub-Plinian eruptions (see Sect. 2), we compare the GSDs of the Avellino (Plinian) and Pollena (sub-Plinian) eruptions (i.e. Figs. 2 and 3). The proximal areas show similar modes (i.e. -3 Φ at ~5 km from the source and between -2 and -1 Φ at ~25 km), proportions and sizes. Furthermore, we compare the proximal GSDs of these eruptions with those of the Pompeii Plinian eruption reported in Macedonio et al. (1988) and collected in Pompeii (~11 km), Castellammare (~15 km), and Maiori (~25 km) respectively. GSDs have modes at -3 Φ, except for Maiori which peaks at -2 Φ, being consistent with the results associated with the Avellino and Pollena eruptions. In the medial zone, samples for the two eruptions located at ~100 km from the source peak at 2 Φ, and those at ~130 km have modes at 5 and 3 Φ (Table 1), respectively for Avellino and Pollena eruptions. According to Sulpizio et al. (2008), this feature indicates that a more intense magma fragmentation with high proportions in fines occurred during the Avellino eruption, especially during the magmatic Plinian phase. The distal modes for the two eruptions peak between 5 and 6 Φ for samples located in the Shkodra lake (Albania; Sulpizio et al., 2010a), indicating relatively the same atmospheric conditions and intensity of magma fragmentation leading to a tephra dispersal towards north-east. It is worth noting that interpreting grain-size relative to fine ash in terms of intensity of fragmentation is complex as the energy released at fragmentation depends on the sum of different contributions and the mechanical strength of the magma (Büttner et al., 2006).

Then we compared the GSDs of the 1906 and 1944 Violent Strombolian eruptions (Figs. 4 and 5), noting that for the proximal and medial areas the tephra fallout appears to be similar in size and proportion for the same sampling sites (i.e. samples 1-7). Nonetheless, the presence of fine ash at very proximal distance from the vent (i.e. < 4 km) suggests the likely occurrence of ash aggregation (Costa et al., 2010; Folch et al., 2010), which appears as disaggregated fine ash at the ground (Mueller et al., 2017). This observation is supported by Arrighi et al. (2001). The modes change in distal areas peaking at 3 and 5 Φ respectively for the 1906 and 1944 eruptions (Table 1), due to different distances from the vent, respectively ~252 and ~460 km. The literature reports the tephra fallout of the 1906 eruption in Montenegro (De Lorenzo, 1906; Barsotti et al., 2015; Fig. 1), but without the possibility of assessing the grain-size distribution due to very thin deposits.

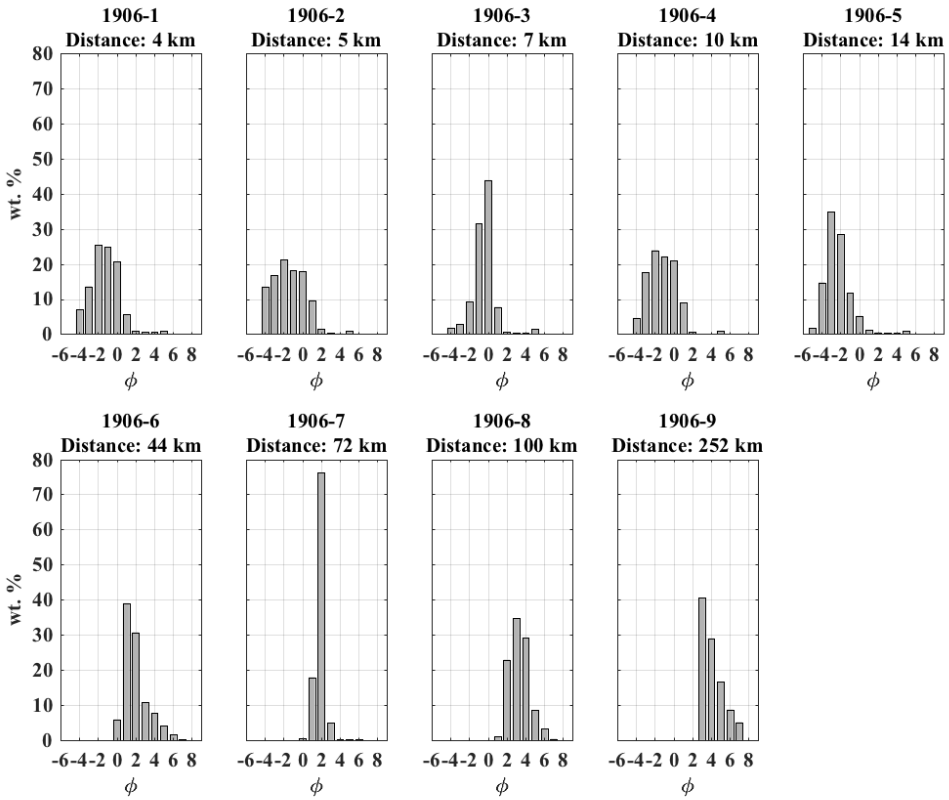

Fig. 4: Individual field grain-size distributions (samples 1906-x) for the 1906 Violent Strombolian eruption. Sample locations are shown in Fig. 1 and the relative details reported in Table 1. Details of the GSDs are available as Supplementary Material (Table S3).

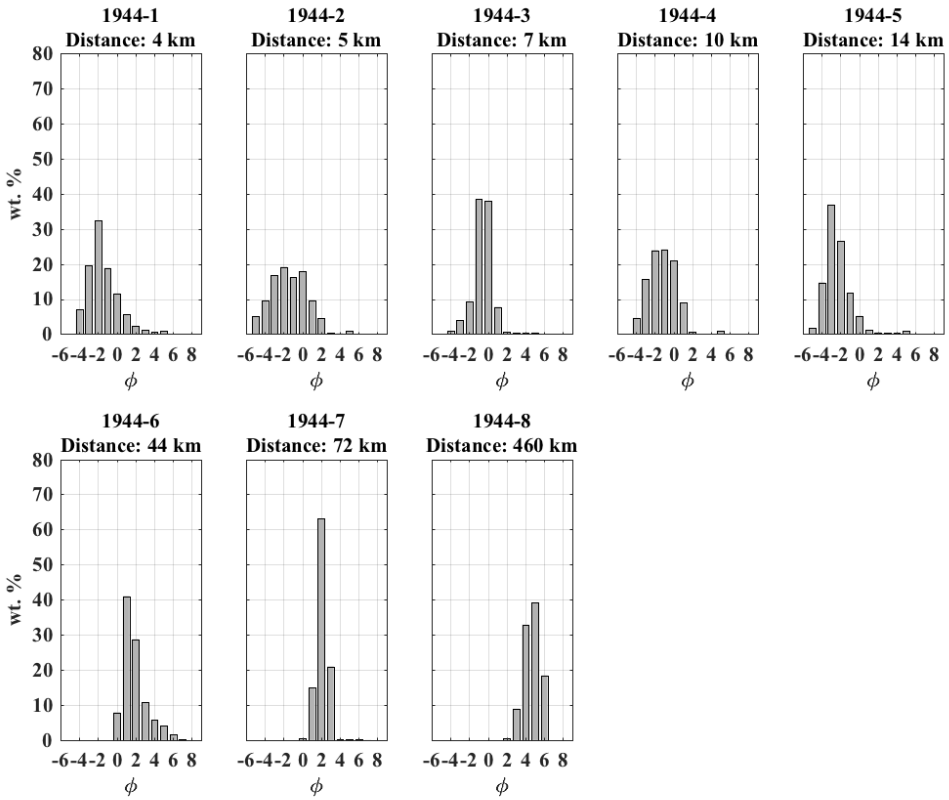

Fig. 5: Individual field grain-size distributions (samples 1944-x) for the 1944 Violent Strombolian eruption. Sample locations are shown in Fig. 1 and the relative details reported in Table 1. Details of the GSDs are available as Supplementary Material (Table S4).

4.2 Total grain-size distributions

In this section, we describe the TGSDs estimated for the studied eruptions by using different methods, such as the Voronoi tessellation method (Bonadonna and Houghton, 2005) or the equivalent bulk grain-size distribution derived from massive PDC deposit (Macedonio et al., 1988; Folch and Sulpizio, 2010), and the analytical parameterizations of the distributions (Costa et al., 2016; 2017). The results give insights into the initial magma fragmentation corresponding to different eruptive styles at Somma-Vesuvius. Although our TGSD estimations are not based on a large number of data in terms of spatial distribution, the dataset covers proximal, medial and distal outcrops for all the studied eruptions. This is quite important as, irrespectively of the eruption style, the lack of distal grain-size data can introduce a significant bias in the TGSD underestimating the fines (e.g. PM_{10}) and, hence, preventing the assessment of the airborne ash, which can pose severe hazards to the air traffic (Guffanti et al., 2005; Folch and Sulpizio, 2010; Sulpizio et al., 2014) and public health (Tomašek et al., 2016; 2018).

As already mentioned, TGSDs are first estimated from field data analysis only (Fig. 6). They indicate an overall bimodality pattern, except for the 1944 eruption. In particular, the Avellino field-derived TGSD peaks at 1 and 4 Φ, respectively for the coarse and fine sub-populations, the Pollena TGSD shows modes at -1 and 6 Φ, and the 1906 TGSD has modes at 0 and 3 Φ. For comparison, the TGSD of the Pompeii Plinian eruption (from Macedonio et al., 2008) peaks at 1 and 5 Φ, in agreement with the TGSDs derived for the Avellino Plinian and Pollena sub-Plinian eruptions. For comparison, the Pollena TGSD estimated assuming an equivalent bulk grain-size distribution derived from massive PDC deposits by Folch and Sulpizio (2010) peaks at 1 and 4-5 Φ, consistently with the estimations made for the Avellino and Pompeii TGSDs. Differently from the other eruptions, the 1944 TGSD yields a unique mode at -2 Φ, more similar to the lower intensity and lower magma viscosity eruptions (Costa et al., 2016). Considering the different eruptive styles of the studied cases, the resulting field-based TGSDs indicate modes shifting towards the fines when the eruption intensity increases, in agreement with the analysis performed in Costa et al. (2016).

The TGSDs estimated through the Voronoi tessellation method were obtained after a careful investigation of the effects of the zero-line contour. In fact, TGSD assessment depends on several factors, such as a suitable number of samples well dispersed along the main tephra dispersal (i.e. proximal, medial, and distal areas), but also on the tephra edge defined as the zero-line (Bonadonna and Houghton, 2005; Bonadonna et al., 2015). For optimizing the TGSD estimate, we used the dispersals of the eruptions available in the literature (see Sect. 2) for constraining the tephra extents for each studied eruption. Volentik et al. (2010) studied the uncertainty related to the position of the zero-line, yielding uncertainties on the standard deviation of the modes and the fine ash contained within the TGSD. Nonetheless, Bonadonna et al. (2015) highlighted that these uncertainties are much higher when tephra deposits are not sampled correctly, i.e. including sites up to distal area.

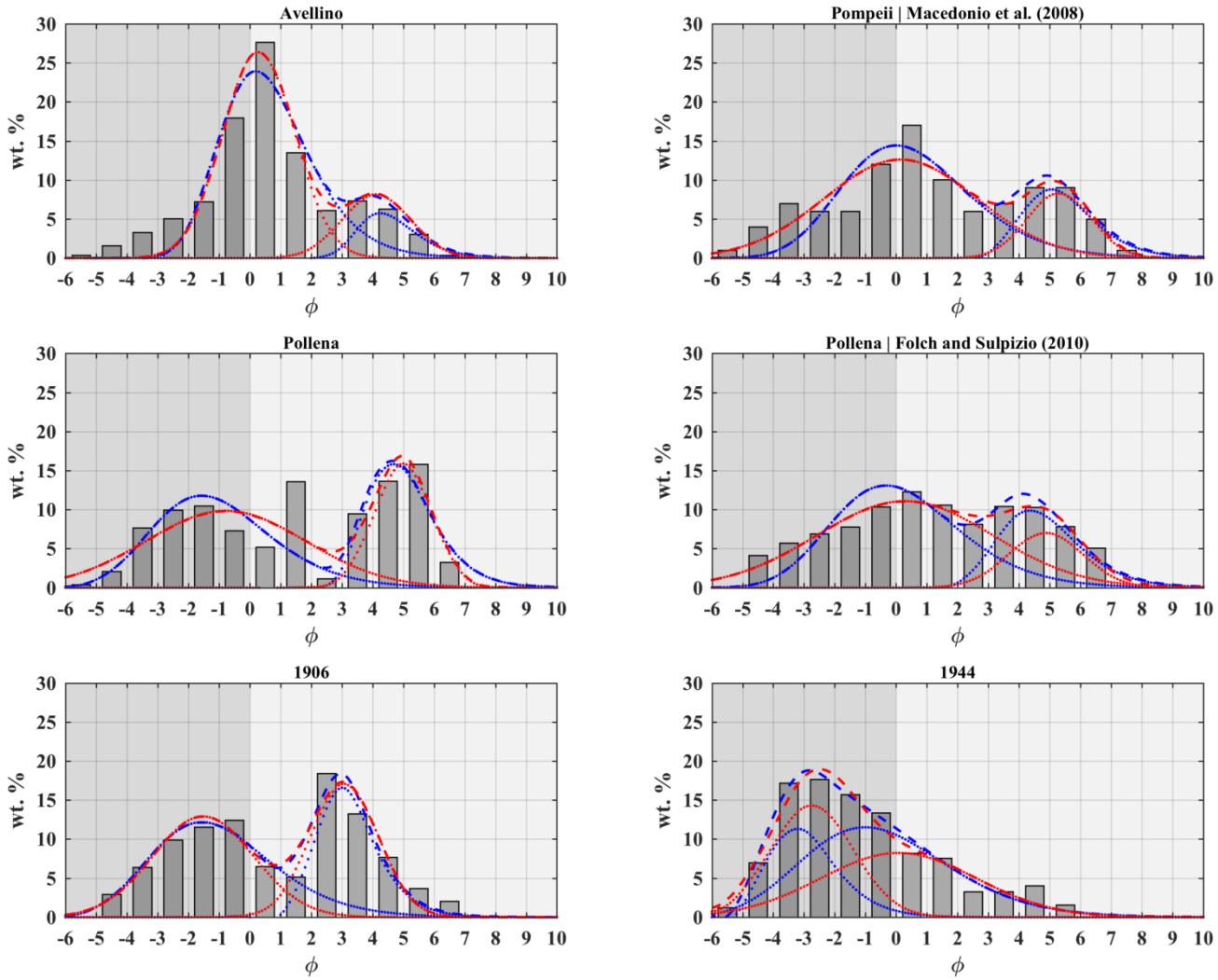

Fig. 6: Field-based TGSDs (bars) for the Avellino, Pollena, 1906, and 1944 eruptions. Red lines show the bi-Gaussian distributions best fitting the field TGSDs, and the blue lines the bi-Weibull distributions. The dotted lines refer to the corresponding sub-populations of the relative distributions. Further details on the distributions in Sect. 3.2, and Tables 2, 3 and 4. The field-based TGSD for the Pompeii eruption is from Macedonio et al. (2008) and is used for comparison with the TGSD of the Avellino eruption. The second field-based TGSD for the Pollena eruption is derived from massive PDC deposits by Folch and Sulpizio (2010) and is used for comparison purpose with the Avellino and Pollena eruptions. Grey colours are consistent with Tables 3 and A (see Appendix).

Among tephra, very fine ash (e.g. PM_{10}) is released into the atmosphere where it can remain for days to weeks dispersing towards distal areas (Rose and Durant, 2009). Such fine material, which escapes to aggregation processes, is very difficult to sample due to the very long residence time in the atmosphere. It follows that PM_{10} are typically under-sampled, biasing the field-derived TGSDs towards the fines and preventing the correct assessment of the airborne ash mass and the relative concentration (Poret et al., 2018a, 2018b), with implications for the assessment of hazards to the air traffic (e.g., Guffanti et al., 2005). In particular, the present study shows that Plinian eruptions (e.g. Avellino and Pompeii) may produce around 80 wt. % of ash with a PM_{10} content of few percent (Table 3), which can have a strong impact on the air traffic safety producing extended areas with ash concentration above the threshold of 4 mg/m^3 (Gouhier et al., 2019 and references therein) delimiting the no-fly zones. It is worth noting that Gouhier et al. (2019) recently demonstrated that the more intense eruptions (i.e. Plinian) are the least efficient in transporting the airborne PM_{10}, due to early en masse fallout. This explains why we regularly observe ash in proximal and medial areas but also suggests that measured PM_{10} fractions are the minimum amount to consider. A few studies have attempted to assess such fraction at Etna (Sicily, Italy) integrating field and remote sensing

data (i.e. satellite and/or X-band radar retrievals; Poret et al., 2018a, 2018b). Although PM_{10} fraction is negligible compared to the bulk tephra, it is critical for operational models (e.g. those used by the Volcanic Ash Advisory Centers) when using the tephra dispersal models.

Considering the time occurrence of the studied eruptions, and the consequent absence of remote sensing data, for trying to better capture the tails of the field-based TGSDs, i.e. fine and coarse, we described the TGSDs by means of bi-Gaussian and bi-Weibull distributions, which allow extrapolations. Overall, all the distributions best fitting the field TGSDs are estimated by assuming two main tephra populations (i.e. a coarse and a fine) as described in Costa et al. (2016; 2017). Indeed, Costa et al. (2016) show that bimodality of TGSDs is a common feature for several tephra fallout deposits. This is also the case of this study, showing asymmetric and clear bimodal signature for all the TGSDs (Fig. 6), except for the 1944 eruption that, although asymmetric, has a more unimodal pattern. However, the obtained TGSDs suggest that bimodality can be due to magma heterogeneity, secondary fragmentation or phreatomagmatism (Jones and Russell, 2017). For better classifying whether TGSDs are bimodal or unimodal, Costa et al. (2016) used a bimodality index (*BI*) for bi-Gaussian distributions as following:

$$BI = \sqrt{2}\frac{|\mu_1 - \mu_2|}{\sqrt{\sigma_1^2 + \sigma_2^2}}\sqrt{p(1-p)}$$

where the parameters μ_i and σ_i refer to modes and standard deviations of the Gaussian distributions (Sect. 3.2). The best fitting parameters are reported in Table 2 together with the associated *BI* values.

Table 2: Parameterization of the distributions in best fit of the field-based TGSDs for the Avellino, Pompeii, Pollena, 1906, and 1944 eruptions. *p* and (1-*p*) are, respectively, the coarse and fine sub-population weights, and μ_1, μ_2 and σ_1, σ_2 are the mean and standard deviation of the two Gaussian distributions in Φ-units. *q* and (1-*q*) are, respectively, the coarse and fine sub-population weights, and λ_1, λ_2 and n_1, n_2 are the scale and shape parameters of the two distributions, respectively. The bimodality is investigated for the Gaussian distributions only through the *BI* (Costa et al., 2016), which is assumed bimodal for *BI* > 1.1. * TGSD is that used from Macedonio et al. (2008) for comparing with the Avellino eruption. ** TGSD is that used by Folch and Sulpizio (2010).

bi-Gaussian						
	Avellino	**Pompeii ***	**Pollena**	**Pollena ****	**1906**	**1944**
μ_1 (Φ)	**0.29 ± 0.07**	**0.14 ± 0.26**	**-0.78 ± 0.46**	**0.28 ± 0.16**	**-1.52 ± 0.17**	**-2.74 ± 0.10**
σ_1 (Φ)	**1.16 ± 0.06**	**2.48 ± 0.21**	**2.60 ± 0.38**	**2.86 ± 0.13**	**1.64 ± 0.14**	**1.34 ± 0.08**
μ_2 (Φ)	**4.12 ± 0.23**	**5.32 ± 0.25**	**4.99 ± 0.17**	**4.87 ± 0.16**	**3.08 ± 0.11**	**0.08 ± 0.24**
σ_2 (Φ)	**1.10 ± 0.19**	**1.04 ± 0.20**	**0.92 ± 0.14**	**1.22 ± 0.13**	**1.10 ± 0.09**	**2.53 ± 0.20**
p	**0.77 ± 0.02**	**0.78 ± 0.03**	**0.63 ± 0.04**	**0.79 ± 0.02**	**0.53 ± 0.03**	**0.48 ± 0.03**
BI	**1.41**	**1.13**	**1.43**	**0.85**	**1.65**	**0.70**
bi-Weibull						
λ_1 (in mm)	**0.41 ± 0.04**	**0.43 ± 0.07**	**1.28 ± 0.31**	**0.54 ± 0.08**	**1.27 ± 0.12**	**4.82 ± 0.28**
n_1	**0.65 ± 0.03**	**0.38 ± 0.01**	**0.42 ± 0.03**	**0.37 ± 0.01**	**0.40 ± 0.01**	**0.95 ± 0.05**
λ_2 (in mm)	**0.03 ± 0.01**	**0.02 ± 0.01**	**0.02 ± 0.01**	**0.02 ± 0.01**	**0.07 ± 0.01**	**0.84 ± 0.07**
n_2	**1.16 ± 0.40**	**0.88 ± 0.15**	**0.98 ± 0.12**	**0.75 ± 0.07**	**1.16 ± 0.06**	**0.30 ± 0.01**
q	**0.86 ± 0.04**	**0.74 ± 0.04**	**0.56 ± 0.05**	**0.68 ± 0.04**	**0.60 ±0.02**	**0.32 ± 0.02**

First of all, the results associated with the bimodal index (*BI*) reported in Table 2 tends to indicate bimodal distributions for all the TGSDs, except for that of the Pollena eruption estimated from Folch and Sulpizio (2010) and the 1944 distribution. Indeed, their values are below 1.1, suggesting a more unimodal distribution, although these distributions are made by coarse and fine populations, which are close enough for showing a unimodal-like shape of the distributions (Fig. 6).

Considering that TGSD is needed as input parameter for tephra dispersal models, typically in the form of discrete size bins, we report the TGSD bins obtained from the field measurements analysis (i.e. Field TGSD) and the corresponding bi-Gaussian and bi-Weibull distributions for the studied eruptions in the Appendix (Tables A1-6). Moreover, we discuss below the magma fragmentation features inferred for each eruption. For the sake of simplicity, Table 3 reports the mass fractions associated with each grain-size class (i.e. bomb, lapilli, coarse, and fine ash).

Putting together the field-based TGSDs and the relative analytical distributions (i.e. bi-Gaussian and bi-Weibull), results for the Avellino eruption suggest a first mode between 0 and 1 Φ and a second mode at 4 Φ, respectively for the coarse and fine sub-populations (Fig. 6; Table A1). The Pollena TGSD shows a first mode from -2 to -1 Φ and a second mode at 5-6 Φ. As described in Sect. 2, the Avellino and Pollena eruptions have similar eruptive trends, even if they are classified as Plinian and sub-Plinian eruptions, respectively. Comparing the relative sub-populations displayed in Fig. 6, the Pollena TGSD indicates a tephra deposit relatively coarser than for Avellino, with a greater production of lapilli (~30 and ~18 wt. % respectively; Tables A1 and A2). In contrast, the Avellino eruption produced substantially more ash than the Pollena one (~80 against ~60 wt. % of ash respectively; Tables A1 and A3), being an indicator of the efficiency of the magma fragmentation. Going further in detail, the Avellino eruption produced more coarse ash with respect to Pollena (~70 vs. ~35 wt. % respectively), whereas the Pollena eruption has more fine ash (~8 vs. ~30 wt. %). Furthermore, the PM_{10} content is greater for the Pollena eruption compared to Avellino (~4 and ~1 wt. % respectively; Tables A1 and A3), indicating either a more efficient magma fragmentation for Pollena, although the eruption showed very unstable eruptive conditions, or a more efficient transport towards distal region, as suggested by Gouhier et al. (2019). It is worth noting that the magmatic phase of the Avellino eruption was accompanied by an energy drop affecting magma fragmentation, representing the phreatomagmatic phase (Sulpizio et al., 2008; 2010b) with a lower fraction of fine ash compare to the Pollena eruption. Sulpizio et al. (2005) explained this as due to magma fragmentation efficiency but also mentioned the occurrence of an extensive magma-water interaction, which occurred during the final phase, carrying out a strong control on the eruption dynamics and increasing the fragmentation of magma during the Pollena eruption.

Going further in the comparative analysis, we compared the Avellino field-derived TGSD with the one of the Pompeii eruption, being both Plinian events. For these purposes, we used the TGSD estimations reported by Macedonio et al. (1988; 2008) for the Pompeii eruption. Macedonio et al. (1988; see Fig. 2b therein) estimated the TGSD from an individual GSD obtained from an outcrop of PDC deposits representative of the collapse of the eruptive column. Concerning the fine ash content, they considered all the bin fractions corresponding to $\Phi \geq 5$ all together as fine residual at $\Phi = 5$. It follows that we consider only the coarse mode that peaks at 1 Φ, being consistent with the Avellino results. Regarding the class fractions, we can see that this TGSD shows a substantial enrichment in lapilli (~37 wt. % against ~18 wt. % respectively; Table 3), and thus, a depletion in ash compared to the Avellino eruption (~63 wt. % against ~82 wt. % respectively). Moreover, it also shows a slight enrichment in fine ash (~14 wt. % against ~10 wt. % respectively). Then, Macedonio et al. (2008) reported the bulk Pompeii TGSD that they assumed representative of the Plinian/Sub-Plinian granulometry at Somma-Vesuvius. We also reconstructed such field-based

TGSD through a bi-Gaussian and bi-Weibull distribution and they are displayed in Fig. 6 for comparing them with the Avellino TGSD. It shows a mode at 0-1 Φ for the coarse population, and at 5 Φ for the fine population (Tables A1-2). Although the paucity of field data implies large uncertainties on the TGSD assessment, the relative TGSDs indicate comparable values for lapilli and ash (Table 3), suggesting acceptable results. Looking at the class fractions, the Pompeii TGSD from Macedonio et al. (2008) shows comparable values with respect to the other TGSDs, with ~24 and ~76 wt. % of lapilli and ash, respectively. Among ash, the TGSD indicates ~52 wt. %, 24 wt. %, and ~6 wt. % of coarse and fine ash, and PM_{10}. It follows that all the three estimates for the Plinian events (i.e. Avellino and Pompeii) are in agreement with a dominancy of ash between 60 and 80 wt. % of the magma fragmentation, being consistent with Rose and Durant (2009) who discussed how silicic eruptions can contain substantial fractions of ash.

Similarly to the previous paragraph, we used the TGSD of the Pollena eruption used by Folch and Sulpizio (2010) for a comparison with our TGSD estimates (see Fig. 6). They obtained the TGSD on the basis of an individual GSD obtained from an outcrop of PDC deposits representative of the collapse of the eruptive column. We also best-fitted their field-based TGSD through the bi-Gaussian and bi-Weibull distributions. The TGSD peaks at 0-1 Φ and 4 Φ for the coarse and fine populations respectively. This is slightly different from our estimate for the Pollena eruption (see Tables A3-4), which can be attributed to a different method for assessing the TGSD. In fact, based on our analysis of the field samples, we obtained a TGSD composed of two more marked grain size populations than for the TGSD of Folch and Sulpizio (2010). In particular, our TGSD suggest a coarser proximal deposit with ~31 wt. % of lapilli instead of ~25 wt. % by Folch and Sulpizio (2010). Regarding the class fractions (Table 3), we can see that Folch and Sulpizio (2010) obtained ~75 wt. % of ash, whereas our TGSD indicates ~69 wt. %. Furthermore, they suggest ~52 wt. %, 23 wt. %, and ~5 wt. % of coarse and fine ash, and PM_{10}, while we have ~37 wt. %, 33 wt. %, and ~3 wt. %, respectively. These results are comparable showing an agreement in favour of saying that during the Pollena eruption magma fragmentation produced around 30 wt. % of lapilli and 70 wt. % of ash, with ~45 wt. % of coarse ash, ~30 wt. % of fine ash, and ~4 wt. % of PM_{10}. In addition, these results are very similar to those of the Plinian eruptions and reinforce the similarity between the Plinian and sub-Plinian eruptive styles.

Table 3: Fractions of the different classes used in this study: bombs ($\Phi \leq -6$), lapilli ($-5 \leq \Phi \leq -1$), and ash ($0 \leq \Phi$). We further distinguish between coarse ($4 \leq \Phi \leq 0$) and fine ash ($\Phi \leq 5$) as described in Folch (2012). We also reported the PM_{10} fraction (diameter below 10 μm) as in Poret et al. (2018b). The fractions are expressed in weight percentage (wt. %) and refer to the field-TGSDs, bi-Gaussian, and bi-Weibull distributions for the Avellino, Pollena, 1906, and 1944 Somma-Vesuvius eruptions. Colours are consistent with Tables A (see Appendix) and Fig. 6. * Pompeii data are extracted from Macedonio et al. (2008) for comparing with the Avellino eruption. ** Pollena data are extracted from Folch and Sulpizio (2010) for comparing with Plinian and sub-Plinian eruptions.

	Class	Field-TGSD	bi-Gaussian	bi-Weibull
Avellino	Bombs	0.00	0.00	0.00
	Lapilli	17.62	18.70	19.71
	Ash	82.38	81.29	80.28
	Coarse ash	72.65	73.14	72.15
	Fine ash	9.73	8.15	8.13
	PM_{10}	0.35	0.29	0.81
	Total	100	100	100
Pompeii *	Bombs	0.00	0.59	0.00
	Lapilli	23.98	30.29	24.80
	Ash	78.28	69.12	75.20
	Coarse ash	52.11	48.77	52.17
	Fine ash	24.17	20.35	23.03
	PM_{10}	6.05	2.95	5.21
	Total	100	100	100
Pollena	Bombs	0.00	1.31	0.12
	Lapilli	30.58	32.53	36.10
	Ash	69.44	66.17	63.79
	Coarse ash	36.71	38.48	35.12
	Fine ash	32.73	27.69	28.67
	PM_{10}	3.26	1.71	4.58
	Total	100	100	100
Pollena **	Bombs	0.00	0.99	0.01
	Lapilli	24.53	29.34	26.89
	Ash	75.12	69.67	73.09
	Coarse ash	51.84	50.80	53.12
	Fine ash	23.28	18.87	19.97
	PM_{10}	5.10	2.93	4.08
	Total	100	100	100
1906	Bombs	0.00	0.31	0.19
	Lapilli	30.78	38.73	38.10
	Ash	69.22	60.95	61.70
	Coarse ash	55.78	56.72	56.48
	Fine ash	13.44	4.23	5.22
	PM_{10}	2.07	0.03	0.40
	Total	100	100	100
1944	Bombs	0.00	1.21	0.42
	Lapilli	58.73	65.92	65.77
	Ash	41.28	32.86	33.80
	Coarse ash	35.66	30.83	31.54
	Fine ash	5.62	2.03	2.26
	PM_{10}	0.02	0.27	0.52
	Total	100	100	100

Regarding the Violent Strombolian eruptions at Somma-Vesuvius, the TGSD reconstructed for the 1906 eruption has a first mode from -2 to 0 Φ for the coarse sub-population, and a second mode at 3 Φ for the fine sub-population (Table 3; Fig. 6). The 1944 TGSD presents significant differences with respect to the 1906 one, showing a unimodal pattern with a main mode between -3 and -2 Φ. Indeed, the second mode is not clearly visible from the Field TGSD, characterizing the fine sub-population and peaking between -1 and 0 Φ (respectively for the bi-Weibull and bi-Gaussian distributions), partially overlapping the coarse sub-population (see Fig. 6). Such discrepancy between the 1906 and 1944 TGSDs can be interpreted as due to the different processes controlling magma fragmentation, such as the higher intensity and the major phreatomagmatic phase of the 1906 eruption (Costa et al., 2016). In fact, these results, together with the features of the Pollena TGSD, support the importance of the phreatomagmatic phase in controlling magma fragmentation (Sulpizio et al., 2010b). As described in Sect. 2.3, the 1906 and 1944 eruptions are similar in terms of eruptive style. Comparing the class fractions, the 1906 TGSD is substantially depleted in lapilli than the 1944 one (~31 and ~59 wt. % respectively; Table 3), but enriched in ash (respectively ~69 and ~41 wt. %; Table 3). Accordingly, the literature (Arrighi et al., 2001) reports that the 1944 event produced a large quantity of lapilli. Another feature reported for the 1944 eruption concerns the production of ash aggregates up to centimetric size (Arrighi et al., 2001). Although aggregation implies a premature tephra fallout (Durant et al., 2009; Mastin et al., 2016; Poret et al., 2018c), it also depletes the TGSD in fines (Poret et al., 2017), affecting the grain-size distribution towards the fine ash. This also depends on the sampling distance from the source as highlighted by Spanu et al. (2016). Comparing coarse and fine ash, the results indicate a greater production for the 1906 compared to the 1944 eruption (respectively ~56 against ~36 wt. % for the coarse ash, and ~13 against ~6 wt. % for the fine ash; Table 3). Furthermore, the PM_{10} fractions yield ~2 wt. % and <1 wt. % for the 1906 and 1944 eruptions, respectively.

Summarizing the TGSD analyses, the results allow identifying distinctive grain-size features for the different eruptive styles at Somma-Vesuvius, although the paucity of field data prevents assuming the reconstructed TGSDs as fully representative of the initial magma fragmentation conditions. Indeed, results generally indicate that increasing in intensity (i.e. from Violent Strombolian to Plinian eruptions) tends to move the main modes of the TGSDs towards the fines (Fig. 6 and Tables A). Such feature was also reported by Costa et al. (2016), who proposed a model for estimating the TGSD through the bulk magma viscosity and column height. They observed the mode shifting towards the fines when increasing the magma viscosity and intensity values. In particular, the Plinian eruptions (e.g. Avellino and Pompeii at Somma-Vesuvius) appear to be the richest in ash with up to ~82 wt. % (Table 3). In addition, the Pollena sub-Plinian eruption with ~70 wt. % of ash (PM_{10} of ~4 wt. %) and the 1906 Violent Strombolian eruption with ~69 wt. % of ash (PM_{10} of ~2 wt. %) show exceptional magma fragmentation efficiency in contrast with the Avellino, Pompeii, and 1944 eruptions.

5 Conclusions

This study presents grain-size analyses obtained from several tephra samples associated with four reference eruptions of Somma-Vesuvius, covering different eruptive styles (from Violent Strombolian to Plinian), aimed to assess the relative TGSD and the impact of magma fragmentation

on the eruptive styles. Chronologically, we focus on the Avellino (3900 yr BP) and the Pompeii (A.D. 79) Plinian eruptions, the Pollena sub-Plinian eruption (A.D. 472), and the 1906 and 1944 Violent Strombolian eruptions. Previous estimations of the Pompeii and Pollena eruptions were used for comparison purposes in terms of magma fragmentation for a given eruptive style. Individual field-based grain-size analyses were integrated using the Voronoi tessellation method for assessing the TGSD relative to each eruption. Besides the estimation of the field-derived TGSDs, we parameterized the TGSDs using the analytical bi-Gaussian and bi-Weibull distributions. By comparing the TGSDs associated with the different eruptive styles, our results indicate that increasing the eruption intensity, i.e. going from Violent Strombolian to Plinian eruptive style, and the efficiency of magma-water interaction, i.e. from magmatic to phreatomagmatic eruptions, TGSD modes move towards the fines, enhancing magma fragmentation. This study brings together similar conclusions in terms of magma fragmentation stated in the literature, reinforcing their findings and reopening the interest of studying the fragmentation from field data but not limited to. We believe this study will serve further works focussing on characterizing the tephra distribution produced by volcanic eruptions worldwide from Violent Strombolian to Sub-Plinian and Plinian styles. In particular, the main findings of this study can be used for numerically reconstructing past eruptions or forecasting similar eruptive scenarios at Somma-Vesuvius, and assessing tephra loading and/or airborne ash mass from the source towards distal regions.

Acknowledgements

This work has been partially supported by the FP 7 Marie Curie Actions Framework (FP7-PEOPLE-2013- ITN), volcanic ash: field, experimental, and numerical investigations of processes during its lifecycles (VERTIGO project; grant agreement number 607905). A.C. acknowledges the European project EUROVOLC (grant agreement number 731070) and the Ministero dell'Istruzione, dell'Università e della ricerca (MIUR, Roma, Italy) Ash-RESILIENCE project (grant agreement number 805 FOE 2015).

Appendix

Table A1: Field-derived TGSD together with the corresponding bi-Gaussian and bi-Weibull distributions for the Avellino Plinian. TGSDs are expressed in weight percentage (wt. %) and displayed in Fig. 6. The related grain-size class fractions are reported in Table 3. Colours are consistent with Fig. 6 and Table 3.

Diameter (Φ)	Field TGSD	bi-Gaussian	bi-Weibull
-6	0.00	0.00	0.00
-5	0.35	0.00	0.00
-4	1.61	0.03	0.00
-3	3.31	0.49	0.26
-2	5.09	3.83	4.07
-1	7.26	14.35	15.38
0	18.00	25.72	23.69
1	27.66	22.17	20.60
2	13.53	10.31	12.46
3	6.13	6.65	7.42
4	7.33	8.29	7.98
5	6.31	5.95	5.28
6	3.07	1.91	2.04
7	0.35	0.27	0.60
8	0.00	0.02	0.16
9	0.00	0.00	0.04
10	0.00	0.00	0.01

Table A2: Field-derived TGSD from Macedonio et al. (2008) together with the corresponding bi-Gaussian and bi-Weibull distributions for the Pompeii Plinian eruption. TGSDs are expressed in weight percentage (wt. %) and displayed in Fig. 6. The related grain-size class fractions are reported in Table 3. Colours are consistent with Fig. 6 and Table 3.

Diameter (Φ)	Field TGSD	bi-Gaussian	bi-Weibull
-6	0.00	0.59	0.00
-5	1.00	1.47	0.10
-4	3.98	3.13	0.80
-3	7.00	5.65	3.32
-2	6.00	8.69	7.97
-1	6.01	11.35	12.61
0	12.03	12.59	14.43
1	17.03	11.88	12.88
2	10.04	9.58	9.49
3	6.01	7.19	6.71
4	7.00	7.53	8.66
5	9.06	9.87	10.54
6	9.07	7.53	7.28
7	5.03	2.53	3.39
8	1.02	0.38	1.27
9	0.00	0.04	0.42
10	0.00	0.00	0.13

Table A3: Field-derived TGSD together with the corresponding bi-Gaussian and bi-Weibull distributions for the Pollena sub-Plinian eruption. TGSDs are expressed in weight percentage (wt. %) and displayed in Fig. 6. The related grain-size class fractions are reported in Table 3. Colours are consistent with Fig. 6 and Table 3.

Diameter (Φ)	Field TGSD	bi-Gaussian	bi-Weibull
-6	0.00	1.31	0.12
-5	0.38	2.63	1.04
-4	2.08	4.56	3.95
-3	7.67	6.81	8.38
-2	9.97	8.77	11.45
-1	10.48	9.76	11.28
0	7.32	9.36	8.70
1	5.18	7.74	5.59
2	13.57	5.61	3.15
3	1.15	4.96	4.03
4	9.49	10.81	13.65
5	13.65	16.86	15.55
6	15.82	9.12	8.54
7	3.26	1.59	3.22
8	0.00	0.11	1.00
9	0.00	0.01	0.28
10	0.00	0.00	0.08

Table A4: Field-derived TGSD from Folch and Sulpizio (2010) together with the corresponding bi-Gaussian and bi-Weibull distributions for the Pollena sub-Plinian eruption. TGSDs are expressed in weight percentage (wt. %) and displayed in Fig. 6. The related grain-size class fractions are reported in Table 3. Colours are consistent with Fig. 6 and Table 3.

Diameter (Φ)	Field TGSD	bi-Gaussian	bi-Weibull
-6	0.00	0.99	0.01
-5	0.00	2.00	0.20
-4	4.14	3.60	1.27
-3	5.70	5.72	4.28
-2	6.92	8.03	8.79
-1	7.76	9.99	12.35
0	10.36	11.00	12.92
1	12.31	10.76	10.78
2	10.59	9.66	8.17
3	8.14	9.18	9.28
4	10.44	10.20	11.97
5	10.33	9.86	10.09
6	7.86	6.08	5.80
7	5.10	2.22	2.60
8	0.00	0.54	1.00
9	0.00	0.13	0.36
10	0.00	0.04	0.12

Table A5: Field-derived TGSD together with the corresponding bi-Gaussian and bi-Weibull distributions for the 1906 Violent Strombolian eruption. TGSDs are expressed in weight percentage (wt. %) and displayed in Fig. 6. The related grain-size class fractions are reported in Table 3. Colours are consistent with Fig. 6 and Table 3.

Diameter (Φ)	Field TGSD	bi-Gaussian	bi-Weibull
-6	0.00	0.31	0.19
-5	0.00	1.35	1.30
-4	2.90	4.11	4.42
-3	6.41	8.59	8.85
-2	9.91	12.38	11.84
-1	11.56	12.30	11.69
0	12.44	8.72	9.15
1	6.53	6.78	6.32
2	5.17	11.81	12.01
3	18.41	17.34	18.40
4	13.23	12.07	10.60
5	7.67	3.70	3.74
6	3.70	0.50	1.08
7	2.07	0.03	0.29
8	0.00	0.00	0.08
9	0.00	0.00	0.02
10	0.00	0.00	0.01

Table A6: Field-derived TGSD together with the corresponding bi-Gaussian and bi-Weibull distributions for the 1944 Violent Strombolian eruption. TGSDs are expressed in weight percentage (wt. %) and displayed in Fig. 6. The related grain-size class fractions are reported in Table 3. Colours are consistent with Fig. 6 and Table 3.

Diameter (Φ)	Field TGSD	bi-Gaussian	bi-Weibull
-6	0.00	1.21	0.42
-5	1.20	4.57	3.14
-4	6.96	11.48	12.88
-3	17.20	18.00	18.68
-2	17.66	18.18	16.98
-1	15.71	13.69	14.09
0	13.36	10.00	11.37
1	8.21	7.98	8.54
2	7.54	6.18	5.85
3	3.26	4.21	3.66
4	3.29	2.46	2.12
5	4.03	1.23	1.15
6	1.57	0.53	0.59
7	0.02	0.19	0.29
8	0.00	0.06	0.14
9	0.00	0.02	0.06
10	0.00	0.00	0.03

References

1. Arrighi, S., Principe, C., and Rosi, M. Violent strombolian and sub-Plinian eruptions at Vesuvius during post-1631 activity. *Bull. Volcanol.* 63, 126–150, doi: 10.1007/s004450100130, 2001.
2. Barsotti, S., Neri, A., Bertagnini, A., Cioni, R., Mulas, M., and Mundula, F. Dynamics and tephra dispersal of Violent Strombolian eruptions at Vesuvius: insights from field data, wind reconstruction and numerical simulation of the 1906 event. *Bull. Volcanol.* 77, 58, doi: 10.1007/s00445-015-0939-6, 2015.
3. Bertagnini, A., Landi, P., Santacroce, R., and Sbrana, A. The 1906 eruption of Vesuvius: from magmatic to phreatomagmatic activity through the flashing of a shallow depth hydrothermal system. *Bull. Volcanol.*, 53, 517–532, 1991.
4. Bertagnini A., Landi P., Rosi M., and Vigliargio A. The Pomici di Base Plinian eruption of Somma-Vesuvius. *J. Volcanol. Geotherm. Res.*, 83, 3, 219–239, 1998.
5. Bonadonna, C., and Houghton, B.F. Total grain-size distribution and volume of tephra-fall deposits. *Bull. Volcanol.* 67, 441–456, doi: 10.1007/s00445-004-0386-2, 2005.
6. Bonadonna, C., and Costa, A. Plume height, volume, and classification of explosive volcanic eruptions based on the Weibull function. *Bull. Volcanol.* 75, 742, doi: 10.1007/s00445-013-0742-1, 2013.
7. Bonadonna, C., Biass, S., and Costa, A. Physical characterization of explosive volcanic eruptions based on tephra deposits: Propagation of uncertainties and sensitivity analysis. *J. Volcanol. Geotherm. Res.* 296, 80–100, doi: 10.1016/j.jvolgeores.2015.03.009, 2015.
8. Büttner, R., Dellino, P., Raue, H., Sonder, I., and Zimanowski, B. Stress-induced brittle fragmentation of magmatic melts: Theory and experiments. *J. Geophys. Res.*, 111, B08204, doi:10.1029/2005JB003958, 2006.
9. Carey, S.N., and Sigurdsson, H. Influence of particle aggregation on deposition of distal tephra from the May 18, 1980, eruption of Mount St-Helens volcano. *J. Geophys. Res.* 87, B8, 7061–7072, doi: 10.1029/JB087iB08p07061, 1982.
10. Cioni, R., Santacroce, R., and Sbrana, A. Pyroclastic deposits as a guide for reconstructing the multi-stage evolution of the Somma-Vesuvius caldera. *Bull. Volcanol.* 60, 207–222, 1999.
11. Cioni, R., Longo, A., Macedonio, G., Santacroce, R., Sbrana, A., Sulpizio, R., and Andronico, D. Assessing pyroclastic fall hazard through field data and numerical simulations: example from Vesuvius. *J. Geophys. Res.* 108, B2, 2063. doi: 10.1029/2001JB000642, 2003a.
12. Cioni, R., Sulpizio, R., and Garruccio, N. Variability of the eruption dynamics during a Subplinian event: the Greenish Pumice eruption of Somma-Vesuvius (Italy). *J. Volcanol. Geotherm. Res.* 124, 1–2, 89–114, doi: 10.1016/S0377-0273(03)00070-2, 2003b.
13. Cioni, R., Gurioli, L., Lanza, R., and Zanella, E. Temperature of the A.D. 79 pyroclastic density current deposits (Vesuvius, Italy). *J. Geophys. Res.* 109, B02207, doi: 10.1029/2002JB002251, 2004.
14. Cioni, R., Bertagnini, A., Santacroce, R., and Andronico, D. Explosive activity and eruption scenarios at Somma-Vesuvius (Italy): towards a new classification scheme. *J. Volcanol. Geotherm. Res.* 178, 331–346, doi: 10.1016/j.jvolgeores.2008.04.024, 2008.
15. Cole, P.D., and Scarpati, C. The 1944 eruption of Vesuvius, Italy: combining contemporary accounts and field studies for a new volcanological reconstruction. *Geol. Mag.* 147, 3, 391–415, doi: 10.1017/S0016756809990495, 2010.
16. Costa, A., Folch, A., and Macedonio, G. A model for wet aggregation of ash particles in volcanic plumes and clouds: 1. Theoretical formulation. *J. Geophys. Res.* 115, B09201. doi:10.1029/2009JB007175, 2010.
17. Costa, A., Pioli, L., and Bonadonna, C. Assessing tephra total grain-size distribution: Insights from field data analysis. *Earth Planet. Sci. Lett.* 443, 90–107, doi: 10.1016/j.epsl.2016.02.040, 2016.
18. Costa, A., Pioli, L., and Bonadonna, C. Corrigendum to "Assessing tephra total grain-size distribution: Insights from field data analysis". [*Earth and Planetary Sci. Lett.* 443, 90–107, 2016]; *Earth and Planetary Sci. Lett.* doi: 10.1016/j.epsl.2017.03.003, 2017.
19. Cubellis, E., Marturano, A., and Pappalardo, L. Le ceneri distali dell'eruzione del Vesuvio del marzo 1944 raccolte a Devoli (Albania). *Quaderni di geofisica* 113, 2013, in italian.
20. De Lorenzo, G. The eruption of Vesuvius in April 1906. *Q. J. Geol. Soc.* 62, 476–483, 1906.
21. Durant, A.J., Rose, W.I., Sarna-Wojcicki, A.M., Carey, S., and Volentik, A.C.M. Hydrometeor-enhanced tephra sedimentation: Constraints from the 18 May 1980 eruption of Mount St. Helens. *J. Geophys. Res.* 114, B03204, doi: 10.1029/2008JB005756, 2009.
22. Durant, A.J., Bonadonna, C., and Horwell, C.J. Atmospheric and Environmental Impacts of Volcanic Particulates. *Elements* 6, 235–240, doi: 10.2113/gselements.6.4.235, 2010.
23. Folch A., Cavazzoni C., Costa A., Macedonio G. An automatic procedure to forecast tephra fallout, J. Volcanol. Geotherm. Res., 177, 767-777, doi:10.1016/j.jvolgeores.2008.01.046, 2008.

24. Folch, A., and Sulpizio, R. Evaluating long-range volcanic ash hazard using supercomputing facilities: application to Somma-Vesuvius (Italy), and consequences for civil aviation over the Central Mediterranean Area. *Bull. Volcanol.* 72, 1039–1059, doi: 10.1007/s00445-010-0386-3, 2010.

25. Folch, A., Costa, A., Durant, A., and Macedonio, G. A model for wet aggregation of ash particles in volcanic plumes and clouds: 2. Model application. *J. Geophys. Res.* 115, B09202. doi:10.1029/2009JB007176, 2010.

26. Folch, A. A review of tephra transport and dispersal models: Evolution, current status, and future perspectives. *J. Volcanol. Geotherm. Res.* 235–236, 96–115, doi: 10.1016/j.volgeores.2012.05.020, 2012.

27. Folch, A., Costa, A., and Basart, S. Validation of the FALL3D ash dispersion model using observations of the 2010 Eyjafjallajökull volcanic ash clouds. *Atmos. Env.* 48, 165–183. doi:10.1016/j.atmosenv.2011.06.072, 2012.

28. Gouhier, M., Eychenne, J., Azzaoui, N., Guillin, A., Deslandes, M., Poret, M., Costa, A., and Husson, P. Low efficiency of large volcanic eruptions in transporting very fine ash into the atmosphere. *Nature Sci. Rep.*, 9, 1449, doi:10.1038/s41598-019-38595-7, 2019.

29. Guffanti, M., Ewert, J.W., Gallina, G.M., Bluth, G.J.S., and Swanson, G.L. Volcanic-ash hazard to aviation during the 2003-2004 eruption activity of Anatahan volcano Commonwealth of the Northern Mariana Islands. *J. Volcanol. Geotherm. Res.* 146, 241–255, doi:10.1016/j.volgeores.2004.12.011, 2005.

30. Gurioli, L., Sulpizio, R., Cioni, R., Sbrana, A., Santacroce, R., Luperini, W., and Andronico, D. Pyroclastic flow hazard assessment at Somma-Vesuvius based on the geological record. *Bull. Volcanol.*, 72, 1021-1038, doi:10.1007/s00445-010-0379-2, 2010.

31. Hobbs, W.H. The grand eruption of Vesuvius in 1906. J Geol 14–7, 636–655, 1906.

32. Imbò, G. L'attività eruttiva e relative osservazioni nel corso dell'intervallo inter-eruttivo 1906–1944 ed in particolare del parossismo del Marzo 1944. *Annali Osservatorio Vesuviano*, V serie, volume unico, 185– 380, 1949, in italian.

33. Jones, T.J., and Russel, J.K. Ash production by attrition in volcanic conduits and plumes. *Nature Sci. Rep.*, 7, 5538, doi:10.1038/s41598-017-05450-6, 2017.

34. Kaminski, E., and Jaupart, C. The size distribution of pyroclasts and the fragmentation sequence in explosive volcanic eruptions. *J. Geophys. Res.* 103, B12, 29759–29779, doi: 10.1029/98JB02795, 1998.

35. Krumbein, W.C. Size Frequency Distribution of Sediments. *J. Sediment. Res.* 4, 2, 65-77, doi: 10.1306/D4268EB9-2B26-11D7-8648000102C1865D, 1934.

36. Macedonio, G., Pareschi, M.T., and Santacroce R. A numerical Simulation of Plinian Fall Phase of 79 A.D. Eruption of Vesuvius. *J. Geophys. Res.* 93, B12, 14817–14827, doi: 10.1029/JB093iB12p14817, 1988.

37. Macedonio, G., Costa, A., and Folch, A. Ash fallout scenarios at Vesuvius: Numerical simulations and implications for hazard assessment. *J. Volcanol. Geotherm. Res.* 178, 3, 366–377, doi: 10.1016/j.jvolgeores.2008.08.014, 2008.

38. Marzocchi, W., Sandri, L., Gasperini, P., Newhall, C., and Boschi E. Quantifying probabilities of volcanic events: The example of volcanic hazard at Mount Vesuvius. *J. Geophys. Res.* 109, B11201, doi:10.1029/2004JB003155, 2004.

39. Massaro, S., Costa, A., and Sulpizio, R. Evolution of the magma feeding system during a Plinian eruption: The case of Pomici di Avellino eruption of Somma-Vesuvius, Italy. *Earth Planetary Sci. Lett.*, 482, 545–555, doi:10.1016/j.epsl.2017.11.030, 2018.

40. Mastin, L.G., Van Eaton, A.R., and Durant, A.J. Adjusting particle-size distributions to account for aggregation in tephra-deposit model forecasts. *Atmos. Chem. Phys.* 16, 9399–9420, doi: 10.5194/acp-16-9399-2016, 2016.

41. Mele, D., Sulpizio, R., Dellino, P., and La Volpe, L. Stratigraphy and eruptive dynamics of a pulsating Plinian eruption of Somma-Vesuvius: the Pomici di Mercato (8900 years B.P.). *Bull. Volcanol.*, 73, 257–278, doi:10.1007/s00445-010-0407-2, 2011.

42. Mueller, S.B., Kueppers, U., Ametsbichler, J., Cimarelli, C., Merrison, J.P., Poret, M., Wadsworth, F.B., and Dingwell, D.B. Stability of volcanic ash aggregates and break-up processes. *Nature – Sci. Rep.* 7, 7440. doi: 10.1038/s41598-017-07927-w, 2017.

43. Mueller, S.B., Houghton, B.F., Swanson, D.A., Fagents, S.A., Klawonn, M., and Poret, M. Total grain-size distribution of a Hawaiian tephra deposit: case study of the 1959 Kīlauea Iki eruption Hawai'i. *Bull. Volcanol.*, xxx, xx–xx, doi:xxxxxxxx, 2019.

44. Murrow, P.J., Rose, W.I., and Self, S. Determination of the total grain size distribution in a Vulcanian eruption column, and its implications to stratospheric aerosol perturbation. *Geophys. Res. Lett.* 7, 11, 893–896, doi: 10.1029/GL007i011p00893, 1980.

45. Neri, A., Aspinall, W.P., Cioni, R., Bertagnini, A., Baxter, P.J., Zuccaro, G., Andronico, D., Barsotti, S., Cole, P.D., Esposito Ongaro, T., Hincks, T.K., Macedonio, G., Papale, P., Rosi, M., Santacroce, R., and Woo, G. Developing an Event Tree for pyroclastic hazard and risk assessment at Vesuvius. *J. Volcanol. Geotherm. Res.*, 178, 397-415, doi:10.1016/j.jvolgeores.2008.05.014, 2008.

46. Pedrazzi, D., Suñe-Puchol, I., Aguirre-Díaz, G., Costa, A., Smith, V.C., Poret, M., Dávila-Harris, P., Miggins, D.P., Hernández, W., and Gutiérrez, E. The Ilopango Tierra Blanca Joven (TBJ) eruption, El Salvador: Volcano-stratigraphy

and physical characterization of the major Holocene event of Central America. *J. Volcanol. Geotherm. Res.*, 377, 81–102, doi:10.1016/j.jvolgeores.2019.03.006, 2019.

47. Perret F.A. The Vesuvius eruption of 1906. Study of a volcanic cycle. *Carnegie Inst Washington Pub* 339, pp 151, 1924.
48. Pesce, A., and Rolandi, G. Vesuvio 1944. L'ultima eruzione, Napoli, *Edizioni Magma*, p. 216, 2000.
49. Poret, M., Costa, A., Folch, A., and Martì, A. Modelling tephra dispersal and ash aggregation: The 26th April 1979 eruption, La Soufrière St. Vincent. *J. Volcanol. Geotherm. Res.* 347, 207–220, doi: 10.1016/j.jvolgeores.2017.09.012, 2017.
50. Poret, M., Corradini, S., Merucci, L., Costa, A., Andronico, D., Vulpiani, G., Montopoli, M., and Freret-Lorgeril, V. Reconstructing volcanic plume evolution integrating satellite and ground-based data: application to the 23 November 2013 Etna eruption. *Atmos. Chem. Phys.* 18, 7, 4695–4714, doi: 10.5194/acp-18-4695-2018, 2018a.
51. Poret, M., Costa, A., Andronico, D., Scollo, S., Gouhier, M., and Cristaldi, A. Modelling eruption source parameters by integrating field, ground-based and satellite-based measurements: The case of the 23 February 2013 Etna paroxysm. *J. Geophys. Res.: Solid Earth* 123, doi: 10.1029/2017JB015163, 2018b.
52. Poret, M. Modelling ash cloud dispersion and the impact of ash aggregation during volcanic eruptions. Thesis, University of Bologna (Italy) *Alma Matter Studiorum*, May 2018, doi:10.13140/RG.2.2.35832.55041, 2018c.
53. Poret, M., Finizola, A., Ricci, T., Ricciardi, G.P., Linde, N., Mauri, G., Barde-Cabusson, S., Guichet, X., Baron, L., Shakas, A., Gouhier, M., Levieux, G., Morin, J., Roulleau, E., Sortino, F., Vasallo, R., Di Vito, M.A., and Orsi, G. The buried boundary of Vesuvius 1631 caldera revealed by present-day diffuse degassing. *J. Volcanol. Geotherm. Res.* 375, 43–56, doi:10.1016/j.jvolgeores.2019.01.029, 2019.
54. Rolandi, G., Bellucci, F., and Cortini, M. A new model for the formation of the Somma Caldera. *Mineral. Petro.* 80, 27–44, doi: 10.1007/s00710-003-0018-0, 2004.
55. Rose, W.I., and Durant, A.J. Fine ash content of explosive eruptions. *J. Volcanol. Geotherm. Res.* 186, 1–2, 32–39, doi: 10.1016/j.jvolgeores.2009.01.010, 2009.
56. Rust, A.C., and Cashman, K.V. Permeability controls on expansion and size distributions of pyroclasts. J. Geophys. Res.116, B11202, doi: 10.1029/2011JB008494, 2011.
57. Sabatini, V. L'eruzione vesuviana dell'Aprile 1906. *Boll. Del R.* Comitato geologico d'Italia, 3, 169–229, 1906, in Italian.
58. Santacroce, R. Somma-Vesuvius. *Quaderni. Ric. Sci.* 114, pp 230, Cons. Naz. delle Ric., Rome, 1987.
59. Santacroce, R., and Sbrana, A. Geological map of Vesuvius at the scale 1:15,000. SELCA editore, Firenze, 2003.
60. Santacroce, R., Cioni, R., Marianelli, P., Sbrana, A., Sulpizio, R., Zanchetta, G., Donahue, D.J., and Joron, J.L. Age and whole rock-glass compositions of proximal pyroclastics from the major explosive eruptions of Somma-Vesuvius: a review as a tool for distal tephrostratigraphy. *J. Volcanol. Geotherm. Res.* 177, 1–18. doi: 10.1016/j.jvolgeores.2008.06.009, 2008.
61. Scandone, R., Iannone, F., and Mastrolorenzo, G. Stima dei parametri dinamici dell'eruzione del 1944 del Vesuvio. Boll. GNV 2, 487–512, 1986.
62. Scandone, R., Giacomelli, L., and Gasparini, P. Mount Vesuvius: 2000 yrs of volcanological observations. *J. Volcanol. Geotherm. Res.*, 58, 263–271, 1993.
63. Scollo, S., Folch, A., and Costa, A. A parametric and comparative study of different tephra fallout models. *J. Volcanol. Geotherm. Res.* 176, 2, 199–211, doi: 10.1016/j.volgeores.2008.04.002, 2008.
64. Scollo, S., Prestifilippo, M., Pecora, E., Corradini, S., Merucci, L., Spata, G., and Coltelli, M. Eruption column height estimation of the 2011–2013 Etna lava fountains. *Annals Geophys.* 57, 2, S0214, doi: 10.4401/ag-6396, 2014.
65. Sevink, J., Van Bergen, M.J., Van der Plicht, J., Feiken, H., Anastasia, C., and Huizinga, A. Robust date for the Bronze Age Avellino eruption (Somma-Vesuvius): 3945 +- 10 cal BP (1995 +- 10 cal BC). *Quat. Sci. Rev.*, 30, 1035-1046, 2011.
66. Sigurdsson, H, Carey, S., Cornell, W., and Pescatore, T. The eruption of Vesuvius A.D. 79. *Nat. Geo. Res.*, 1, 3, 332–387, 1985.
67. Spanu, A., De Vitturi, M.M., and Barsotti, S. Reconstructing eruptive source parameters from tephra deposit: A numerical study of medium-sized explosive eruptions at Etna volcano. *Bull. Volcanol.* 78, 9, 59, doi: 10.1007/s00445-016-1051-2, 2016.
68. Sulpizio, R., Mele, D., Dellino, P., and La Volpe, L. A complex, Subplinian-type eruption from low-viscosity, phonolitic to tephriphonolitic magma: the AD 472 (Pollena) eruption of Somma- Vesuvius, Italy. *Bull. Volcanol.* 67, 743–767, doi: 10.1007/s00445-005-0414-x, 2005.
69. Sulpizio, R., Mele, D., Dellino, P., and La Volpe, L. Deposits and physical properties of pyroclastic density currents during complex Subplinian eruptions: the AD 472 (Pollena) eruption of Somma-Vesuvius, Italy. *Sedimentology* 54, 3, 607–635, doi: 10.1111/j.1365-3091.2006.00852.x, 2007.

70. Sulpizio, R., Caron, B., Giaccio, B., Paterne, M., Siani, G., Zanchetta, G., and Santacroce, R. The dispersal of ash during explosive eruptions from central volcanoes and calderas: an underestimated hazard for the Central Mediterranean area. *IOP Publishing*, Collapse Calderas Workshop, Series 3, doi: 10.1088/1755-1307/3/1/012031, 2008.

71. Sulpizio, R., Van Welden, A., Caron, B., and Zanchetta, G. The Holocene tephrostratigraphic record of Lake Shkodra (Albania and Montenegro). *J. Quat. Sci.* 25, 5, 633–650, doi:10.1002/jqs.1334, 2010a.

72. Sulpizio, R., Cioni, R., Di Vito, M.A., Mele, D., Bonasia, R., and Dellino, P. The Pomici di Avellino eruption of Somma-Vesuvius (3.9 ka BP) part I: stratigraphy, compositional variability and eruptive dynamics. *Bull. Volcanol.* 72, 539–558, doi:10.1007/s00445-009-0339-x, 2010b.

73. Sulpizio, R., Bonasia, R, Dellino P, Mele, D., Di Vito, M.A., and La Volpe, L. The Pomici di Avellino eruption of Somma-Vesuvius (3.9 ka BP) part II: sedimentology and physical volcanology of pyroclastic density current deposits. *Bull. Volcanol.* 72: 559–577, doi:10.1007/s00445-009-0340-4, 2010c.

74. Sulpizio, R., Zanchetta, G., D'Orazio, M., Vogel, H., and Wagner, B. Tephrostratigraphy and tephrochronology of lakes Ohrid and Prespa, Balkans. *Biogeosciences* 7, 3273–3288, doi: 10.5194/bg-7-3273-2010, 2010d.

75. Sulpizio, R., Folch, A., Costa, A., Scaini, C., and Dellino, P. Hazard assessment of far-range volcanic ash dispersal from a violent Strombolian eruption at Somma-Vesuvius volcano, Naples, Italy: implications on civil aviation. *Bull. Volcanol.* 74, 2205–2218, doi: 10.1007/s00445-012-0656-3, 2012.

76. Sulpizio, R., Zanchetta, G., Caron, B., Dellino, P., Mele, D., Giaccio, B., Insinga, D., Paterne, M., Siani, G., Costa, A., Macedonio, G., and Santacroce, R. Volcanic ash hazard in the Central Mediterranean assessed from geological data. *Bull. Volcanol.* 76, 866, doi: 10.1007/s00445-014-0866-y, 2014.

77. Tomašek, I., Horwell, C.J., Damby, D.E., Barošová, H., Geers, C., Petri-Fink, A., Rothen-Rutishauser, B., and Clift, M.J.D. Combined exposure of diesel exhaust particles and respirable Soufrière Hills volcanic ash causes a (pro-)inflammatory response in an in vitro multicellular epithelial tissue barrier model. *Particle and Fibre Toxicology* 13, 1, 67, doi: 10.1186/s12989-016-0178-9, 2016.

78. Tomašek, I., Horwell, C.J., Bisig, C., Damby, D.E., Comte, P., Czerwinski, J., Petri-Fink, A., Clift, M.J.D., Drasler, B., and Rothen-Rutishauser, B. Respiratory hazard assessment of combined exposure to complete gasoline exhaust and respirable volcanic ash in a multicellular human lung model at the air-liquid interface. *Env. Pollution* 238, 977–987, doi: 10.1016/j.envpol.2018.01.115, 2018.

79. Vogel, H., Zanchetta, G., Sulpizio, R., Wagner, B., and Nowaczyk, N. A tephrostratigraphic record for the last glacial–interglacial cycle from Lake Ohrid, Albania and Macedonia. *J. Quat. Sci.* 25, 3, 320-338, doi: 10.1002/jqs.1311, 2009.

80. Volentik, A.C.M., Bonadonna, C., Connor, C.B., Connor, L.J., and Rosi, M. Modeling tephra dispersal in absence of wind: Insights from the climactic phase of the 2450 BP Plinian eruption of Pululagua volcano (Ecuador). *J. Volcanol. Geotherm. Res.*, 193 (1–2), 117–136, 2010.

81. Walker, G.P.L., 1981. The Waimihia and Hatepe plinian deposits from the rhyolitic Taupo Volcanic Centre. *New Zealand J. Geol. Geophys.* 24, 3, 305–324, 1981.

82. Watt, S.F.L., Gilbert, J.S., Folch, A., and Phillips, J.C. An example of enhanced tephra deposition driven by topographic induced atmospheric turbulence. *Bull. Volcanol.* 77, 35, doi: 10.1007/s00445-015-0927-x, 2015.